Several Quantum-Optical Analogies in Coupled Nanoantenna, Waveguide and Metasurface

Jun-Jun Xiao

Harbin Institute of Technology, Shenzhen Graduate School

Xili, Shenzhen 518055, Guangdong Province, China

E-mail: eiexiao@hitsz.edu.cn

IAS Winter School & Workshop on Advanced Concepts in Wave Physics: Topology and Parity-Time Symmetries, HKUST (2016.01.10-15)

Abstract Engineered photonic waveguides have provided in the past decade an extremely rich laboratory tool to visualize with optical waves the classic analogues of a wide variety of coherent quantum phenomena encountered in atomic, molecular or condensed-matter physics. As compared to quantum systems, optics offers the rather unique advantage of a direct mapping of the wave function evolution in coordinate space by simple fluorescence imaging or scanning tunneling optical microscopy techniques. In this contribution recent theoretical and experimental advances in the field of quantum-optical analogies are reviewed. Special attention is devoted to some relevant optical analogies based on the use of curved photonic structures, including: coherent destruction of tunneling in driven bistable potentials; coherent population transfer and adiabatic passage in laser-driven multilevel atomic systems; quantum decay control and Zeno dynamics; electronic Bloch oscillations and Zener tunneling, Anderson localization and dynamic localization in crystalline potentials.

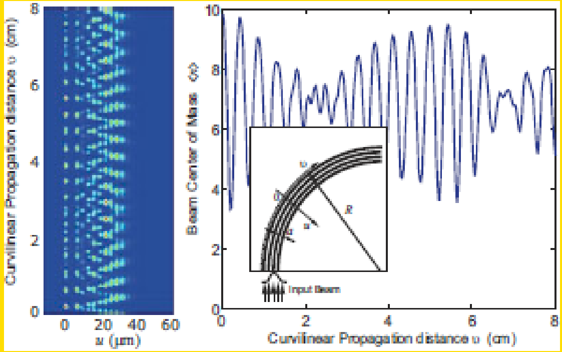

Optical analogue of quantum particle bouncing on a lattice under the gravitational field. A light wave packet periodically bounces the edge of a circularly-curved waveguide array, showing collapses and revivals.

Quantum-optical analogies using photonic structures

*Stefano Longhi**

Dipartimento di Fisica del Politecnico di Milano and Istituto di Fotonica e Nanotecnologie del Consiglio Nazionale delle Ricerche, Piazza Leonardo da Vinci 32, 20133 Milano, Italy

Received: 25 September 2008, Accepted: 13 October 2008
Published online: 9 December 2008

Key words: Quantum-optical analogies, wave optics and wave mechanics, light propagation in coupled optical waveguides and photonic lattices, optical tunneling.

PACS: 42.25.Bs, 42.25.-p, 42.79.Gn

Quantum-Optical Analogues

- Anderson localization
- Zeno resonance
- Fano resonance
- EIT
- Toroidal moment
- Bloch oscillation
- PT-symmetry optics
- Optical topology Insulator
- Spin-dependent optics
- Gauge field optics
- ⋮

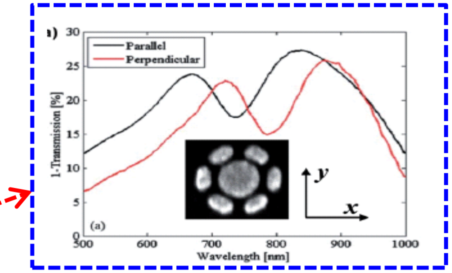

Tamma et al., Nanoscale 5, 1592 (2013)

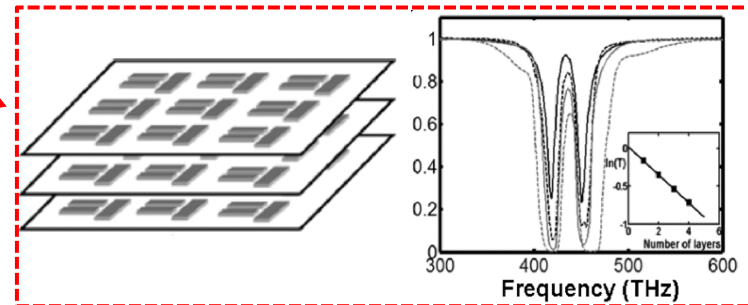

Zhang et al., Phys. Rev. Lett. 101, 047401 (2008)

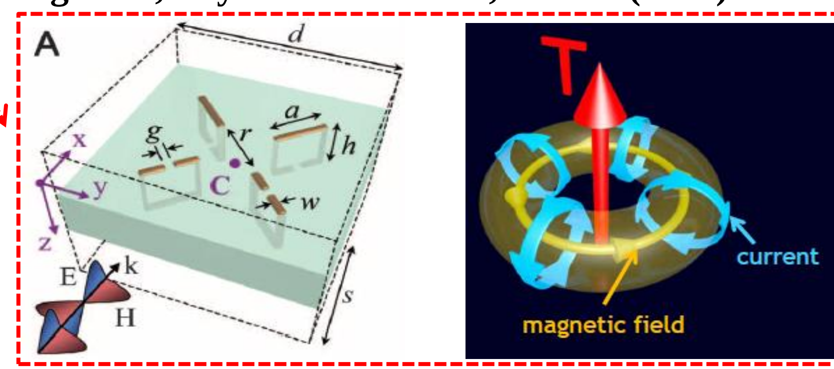

Kaelberer et al., Science 330, 1510 (2010)

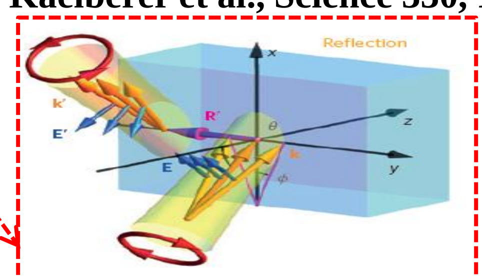

Bliokh et al., Nat. Photonics 9, 796 (2015)

Outline

- **Bloch oscillation in coupled nanoparticles and waveguides**
  - Wave-packet oscillation in time domain
  - Bloch oscillation in spatial domain
- **Fano resonance and EIT in nanoantenna and plasmonic waveguides**
  - Multiple Fano resonances by different order of electric antenna modes
  - Magnetic and toroidal cavity modes in MDM nanodisk
  - Double-EIT in plasmonic slot waveguides
  - Controllable Fano/EIT in plasmonic-dielectric hybrid antenna
- **PT-symmetry optics in coupled waveguides**
  - Absence of EP in finite-size waveguide array of apparently balanced gain/loss
- **Summary**

I. Bloch Oscillation, Fano Resonance & EIT

Wave oscillation in graded nanoparticle chain

$$\widetilde{T}_{nm} = \frac{1}{\epsilon_h(x_n)}(\nabla_n\nabla_n + k^2\mathbf{I})\frac{e^{ik|x_n-x_m|}}{|x_n-x_m|},$$

$$\psi(x,0) = \frac{1}{(2\pi\sigma_x^2)^{1/4}}\exp\left[-\frac{(x-x_0)^2}{4\sigma_x^2}\right]e^{-ik_0x}, \qquad T_B = \frac{2\pi}{f} \approx \frac{2\pi N(2\epsilon_l + c + \xi)^{3/2}}{c\sqrt{\eta}\,\omega_p}.$$

$$|\psi(t)\rangle = \sum_n A_n|\phi_n\rangle e^{i\omega_n t}.$$

~ 11.8 ps

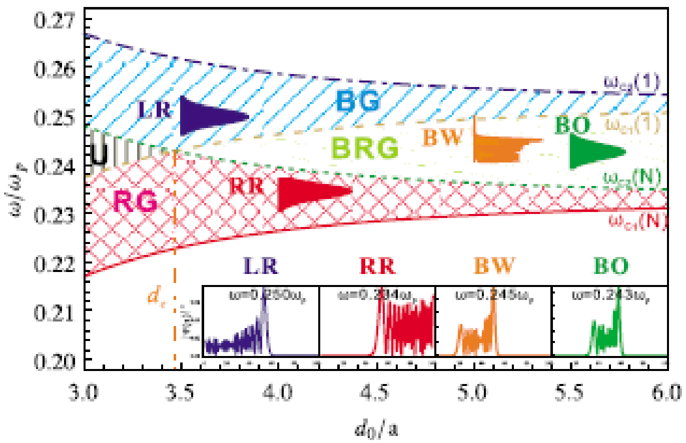

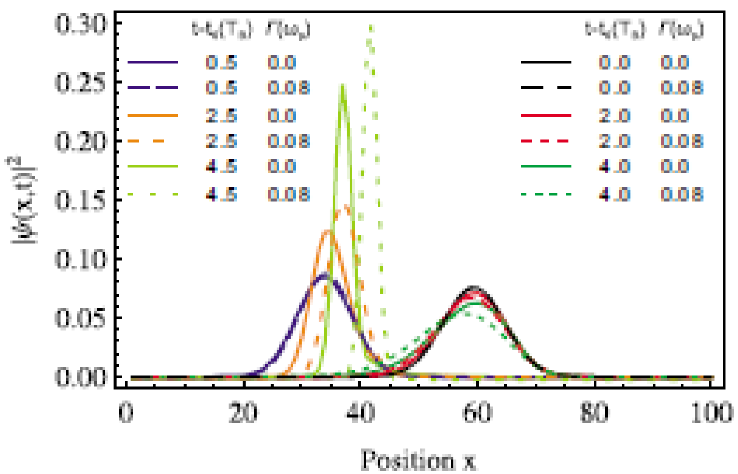

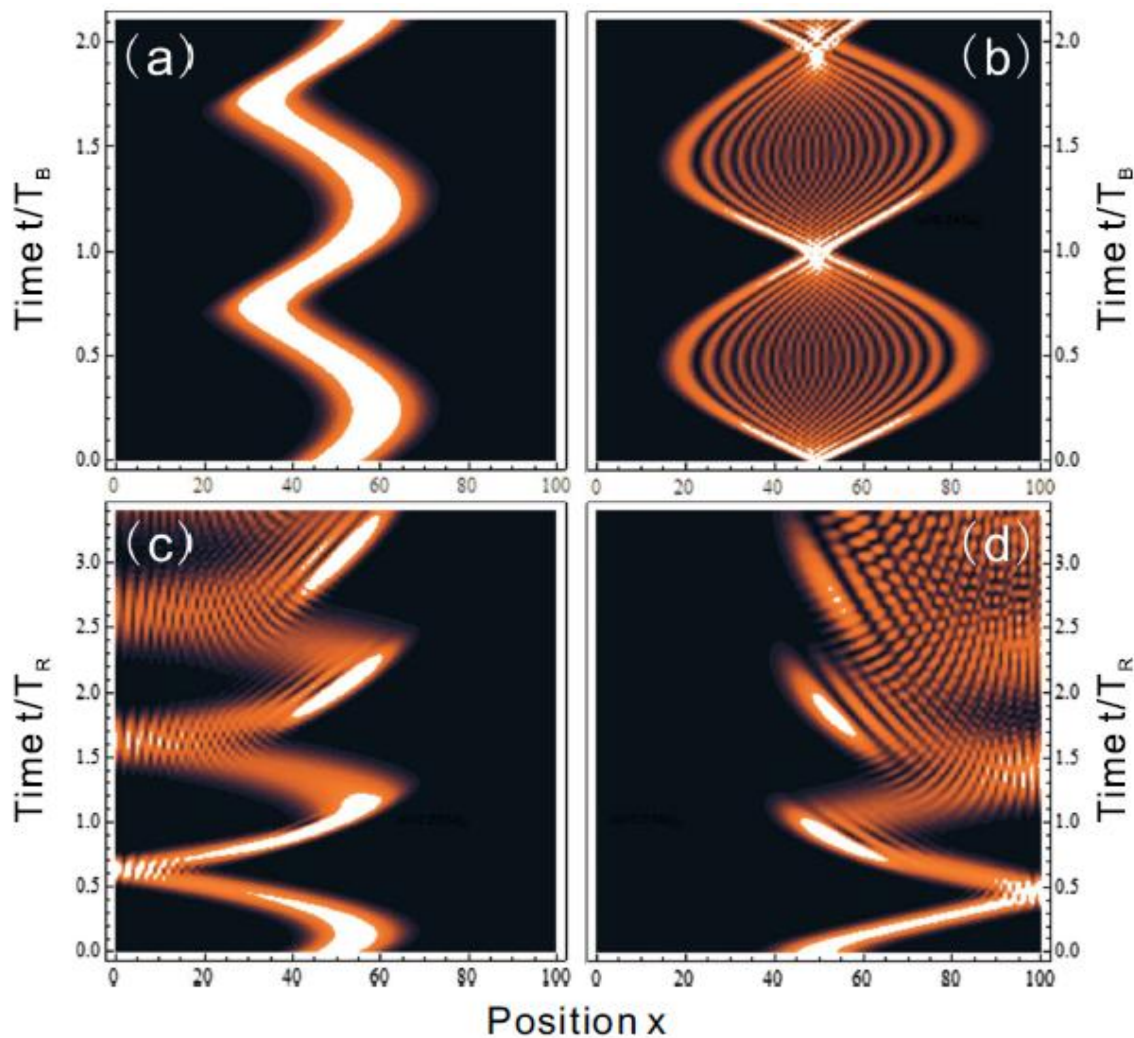

Zheng et al., J. App. Phys. 106, 113307 (2009)

Bloch oscillation in graded waveguide array

$$\left(i\frac{d}{dz}+\alpha n\right)a_n(z)+a_{n+1}(z)+a_{n-1}(z)=0,$$

$$(n=1,2,\ldots,N),$$

Equation of motion:

$$|\psi(0)\rangle=\sum_m A_m|u_m\rangle,$$

$$|\psi(z)\rangle=\sum_m A_m e^{i\beta_m z}|u_m\rangle.$$

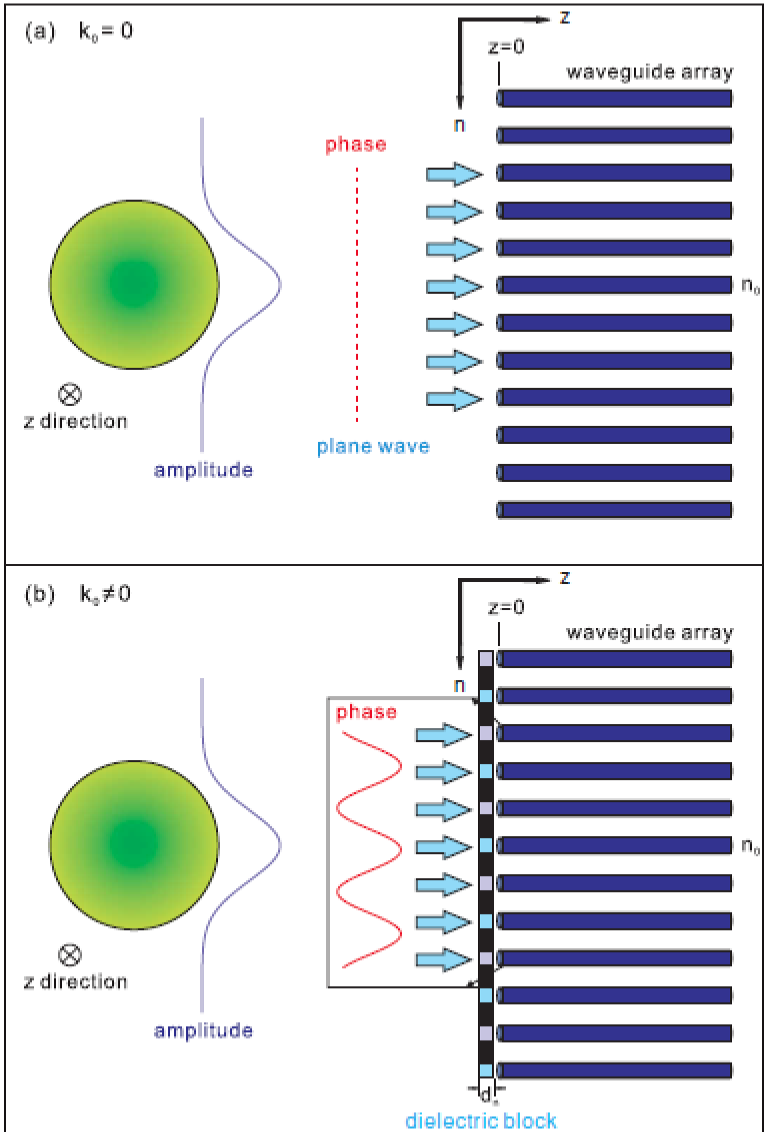

Bloch Oscillation Breathing-like Oscillation

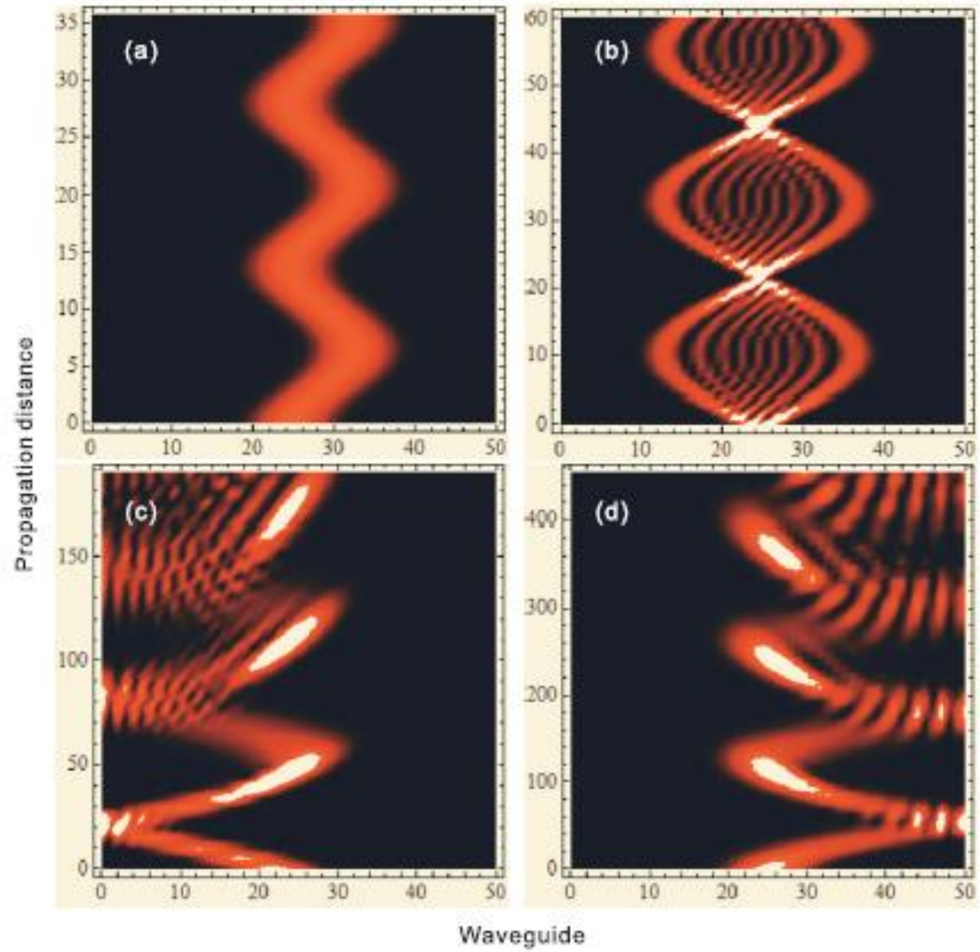

Zheng et al., Phys. Rev. A 81, 033829 (2010)

Classical analogy of Fano resonance & EIT

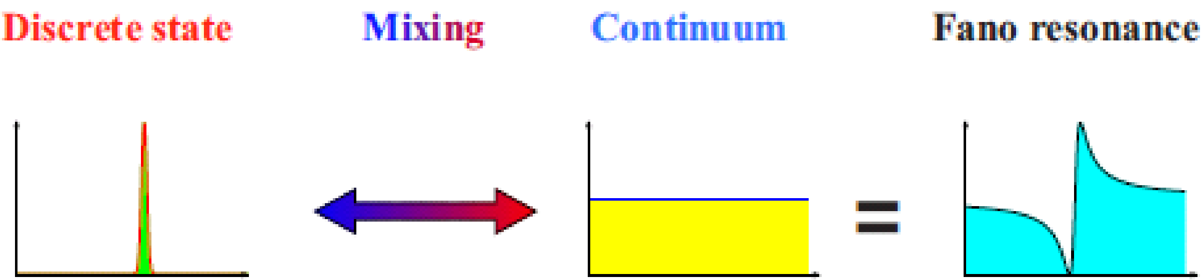

Interference between "bright" and "dark" modes

$$\frac{q^2-1}{\epsilon^2+1} + \frac{2q\epsilon}{\epsilon^2+1} + 1 = \frac{(\epsilon+q)^2}{\epsilon^2+1}$$

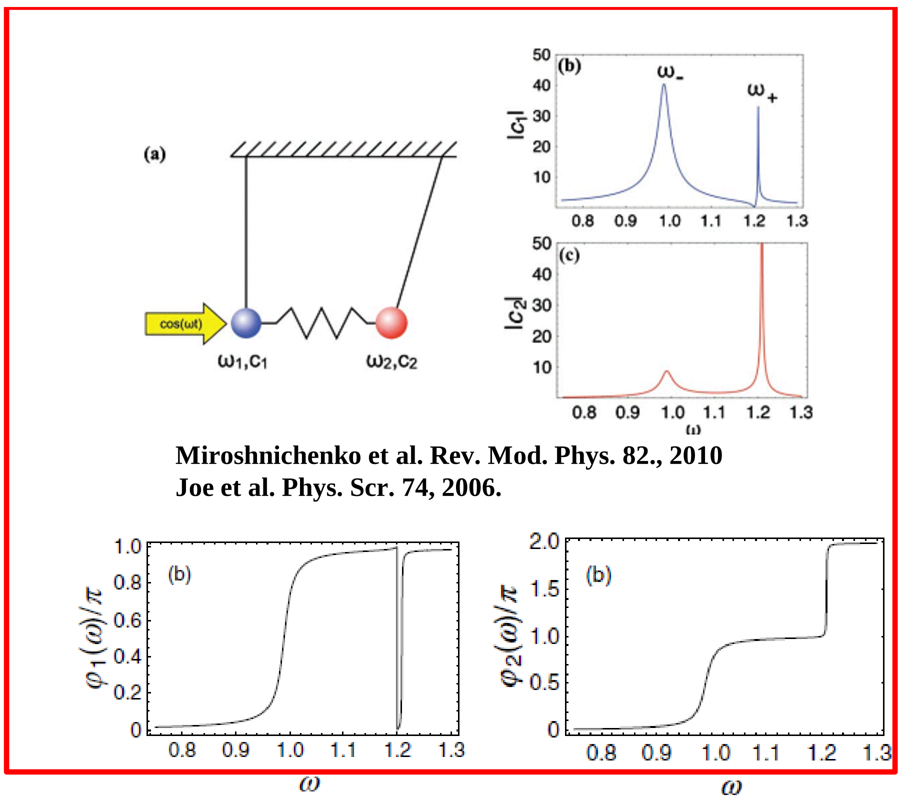

Miroshnichenko et al. Rev. Mod. Phys. 82., 2010
Joe et al. Phys. Scr. 74, 2006.

$$c_1 = \frac{\left(f_2^2 - f^2 + i\gamma_2 f\right)}{\left(f_1^2 - f^2 + i\gamma_1 f\right)\left(f_2^2 - f^2 + i\gamma_2 f\right) - \mu^2} A$$

1. At the Fano dip resonance, the "bright mode" is suppressed
2. Fano dip shows up near the "dark mode" intrinsic frequency
3. Cross the Fano dip, "bright mode" has abrupt phase variation

U. Fano, Phys. Rev. 124, 1866 (1961)

Fano resonance induced by antenna modes

-- Reversal of optical binding force

Homodimer:

---no Fano resonance

---no force reversal

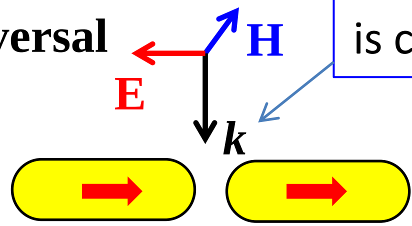

Anti-bonding mode is completely dark

Heterodimer:

----ED-EQ Fano resonance

----Reversal of binding force

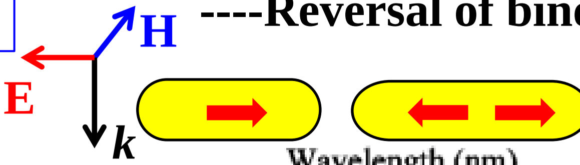

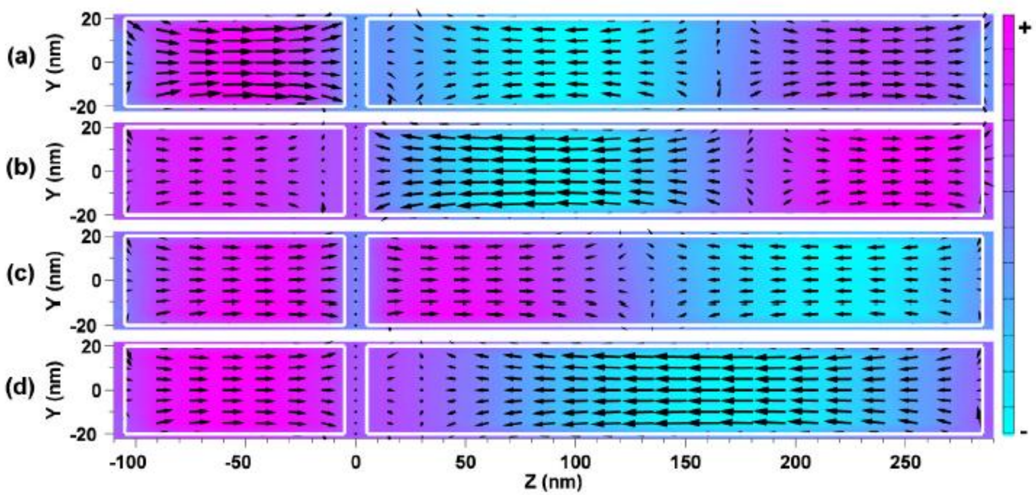

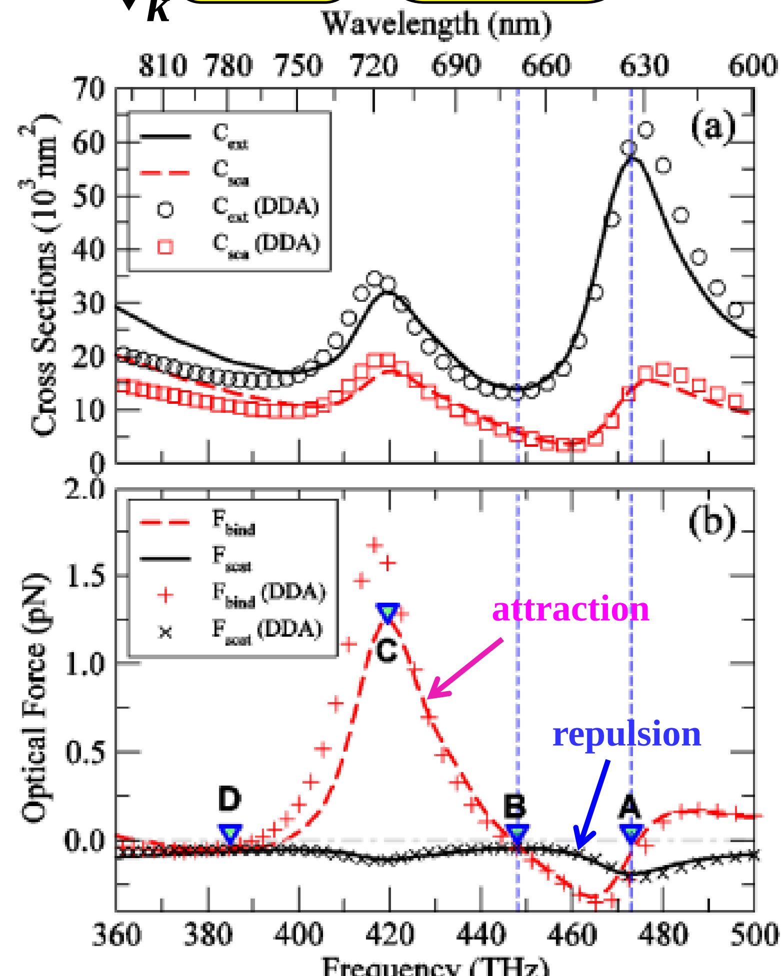

Q. Zhang et al, Opt. Express 21, 6601 (2013)

Multipole Fano resonances induced multiple BF reversals

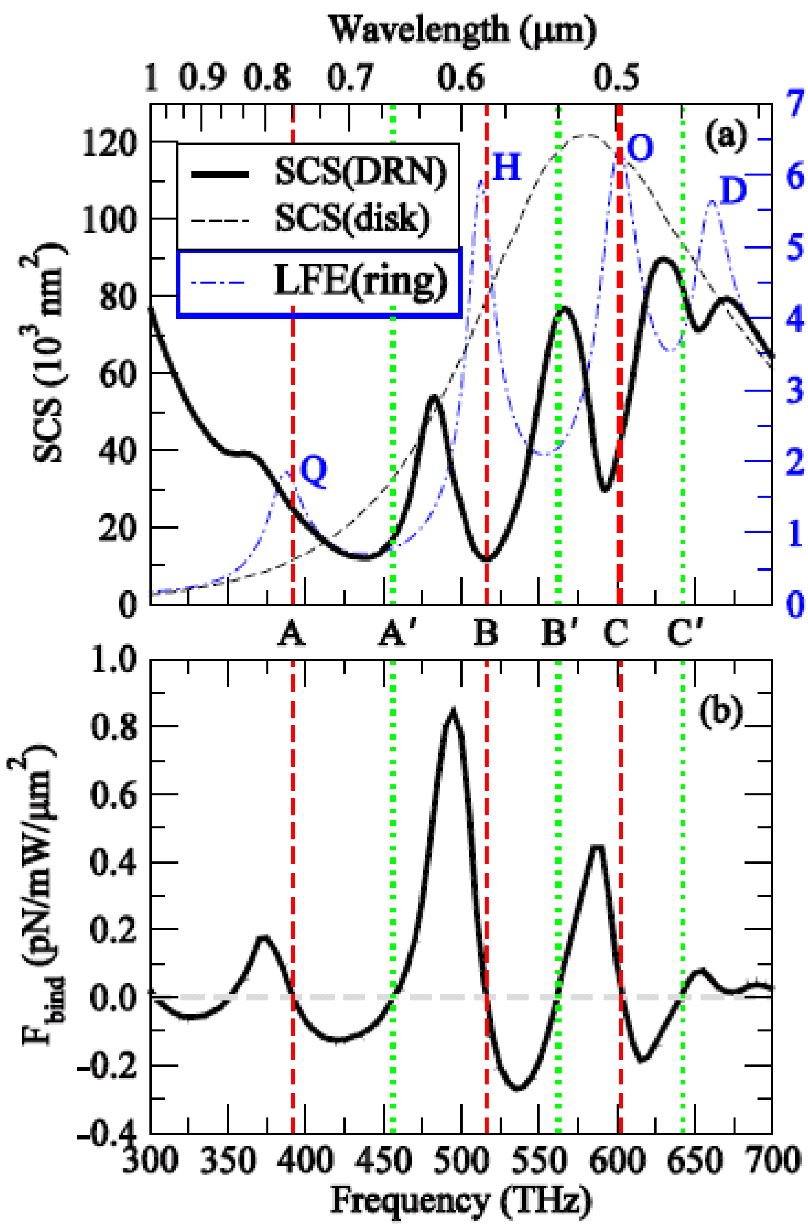

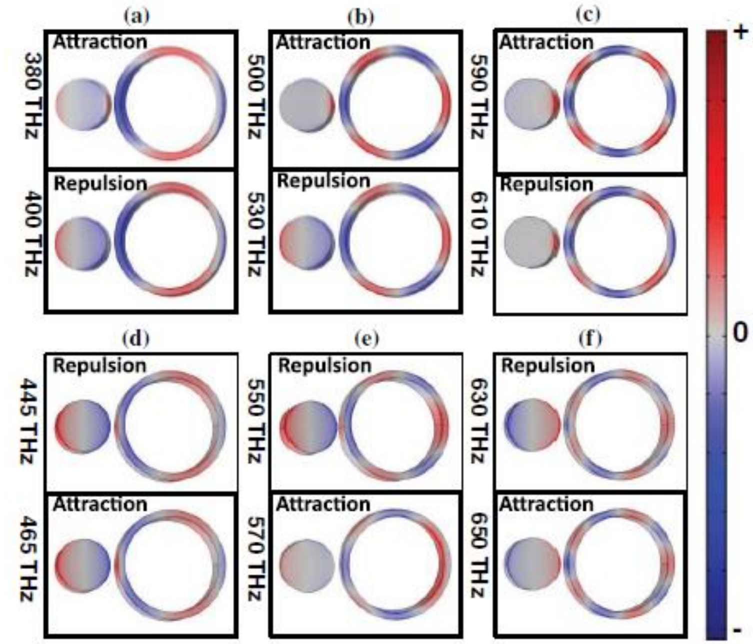

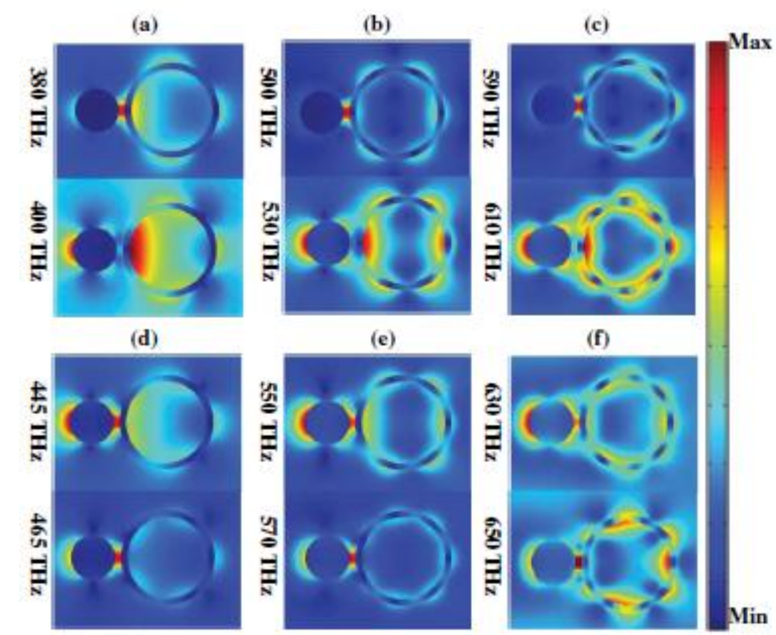

Q. Zhang et al, Opt. Lett. 38, 4240 (2013)

Composite spoof localized surface plasmon (LSP)

Spatially compact while spectrally efficient

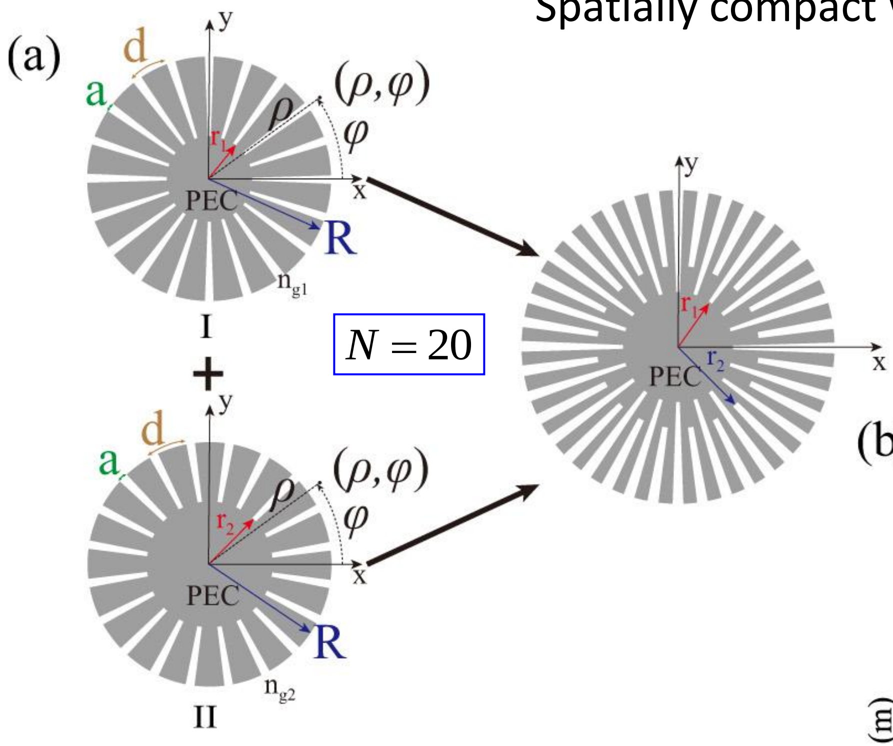

$N = 20$

The spoof LSP resonance modes in the composite resonator are derived from those generated by the substructures

$n_{g1} = n_{g2} = 9.0$

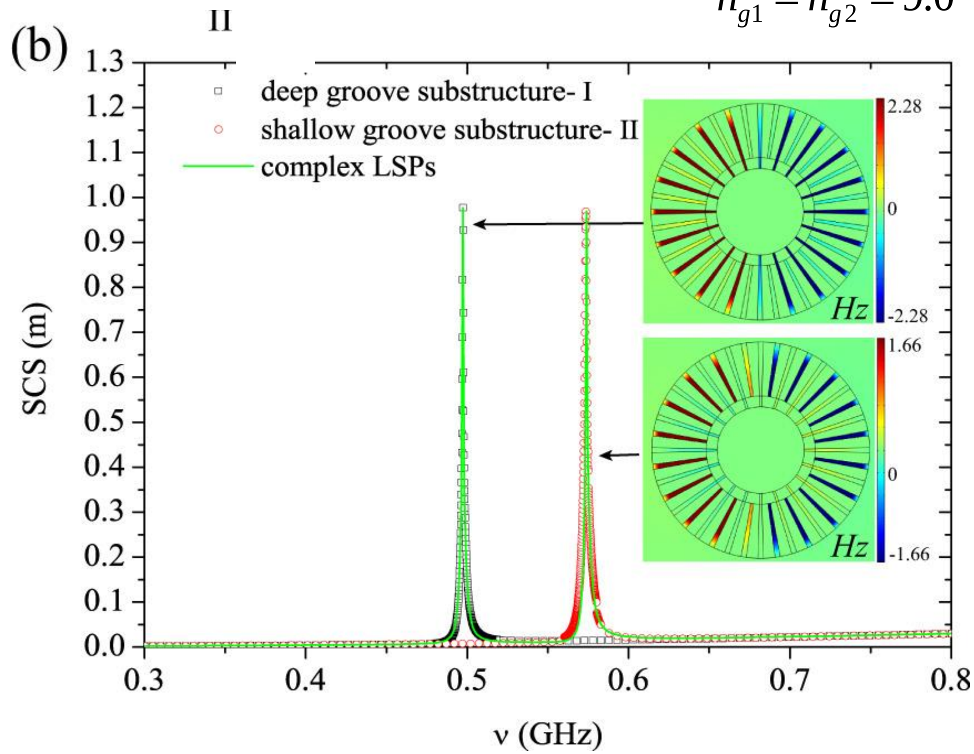

$$\mathrm{R} = 33\,\mathrm{mm}$$

$$d = 2\pi R / N$$

$$a = 0.15d$$

$$r_1 = 0.4R$$

$$r_2 = 0.5R$$

Fano resonance in 2D composite spoof LSPs

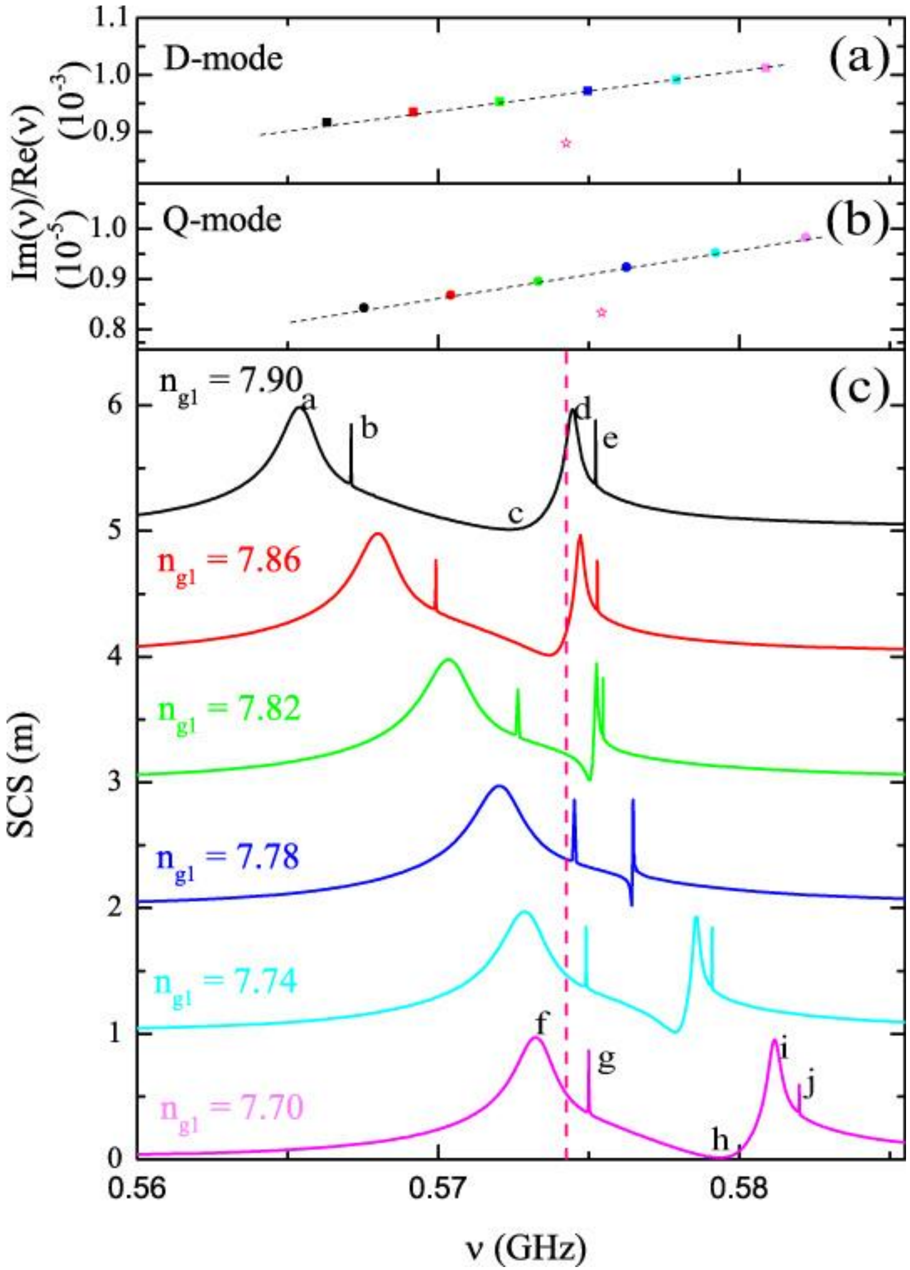

Complex resonance frequencies for the two substructures are calculated

$$S_n^2 \frac{H_n^{(1)}(k_0R)}{H_n^{(1)'}(k_0R)} \frac{f}{g} = n_g$$

$$S_n = \sqrt{a/d}\,\mathrm{sinc}(na/(2R))$$

$$f = J_1(k_0n_gr)Y_1(k_0n_gR) - J_1(k_0n_gR)Y_1(k_0n_gr)$$

$$g = J_0(k_0n_gR)Y_1(k_0n_gr) - J_1(k_0n_gr)Y_0(k_0n_gR).$$

A. Pors et al., Phys. Rev. Lett. 108, 223905 (2012)

The relatively broad D-modes of the two substructures interact with each other and give rise to Fano-like asymmetric line shape in the spectrum

Qin, Xiao and Zhang et al., Opt. Lett. 41, 60 (2016)

Multimode competition and spectrum squeezing

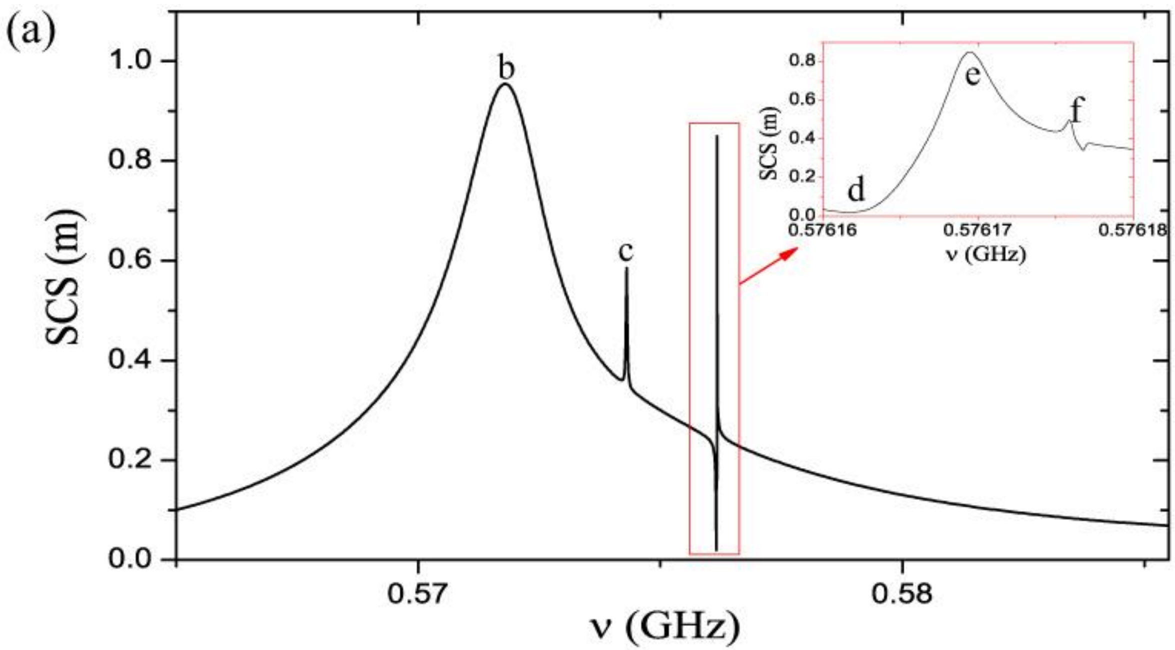

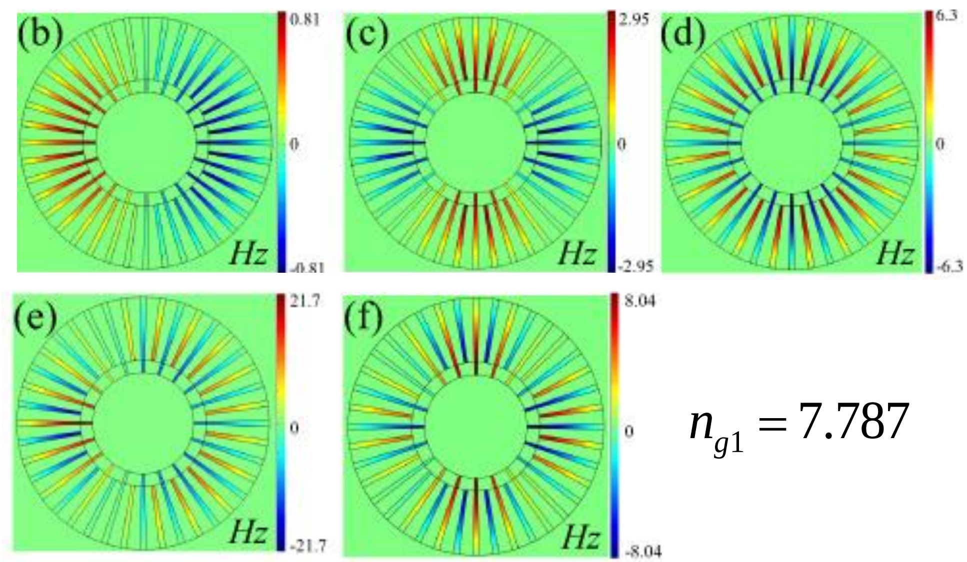

At this particular point, two dipole and one quadrupole resonance of the two substructures come into play, the effect of the quadrupole resonance cannot be neglected

$$n_{g1} = 7.787$$

Fano resonance for 3D complex spoof LSPs (finite thickness)

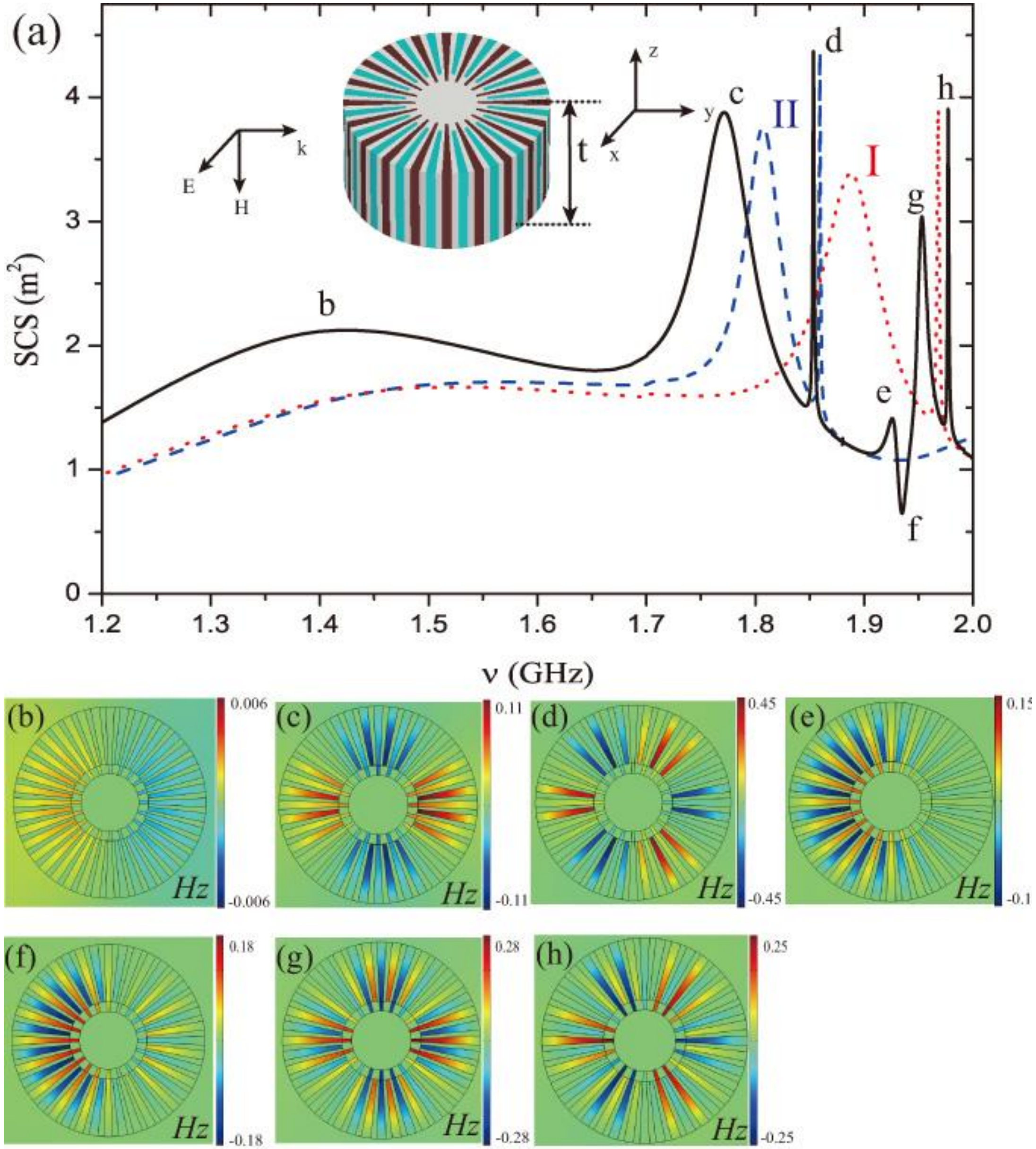

$r_1 = 0.3R$

$r_2 = 0.4R$

$a = 0.3d$

$t = R$

$n_{g1} = 2.9$

$n_{g2} = 2$

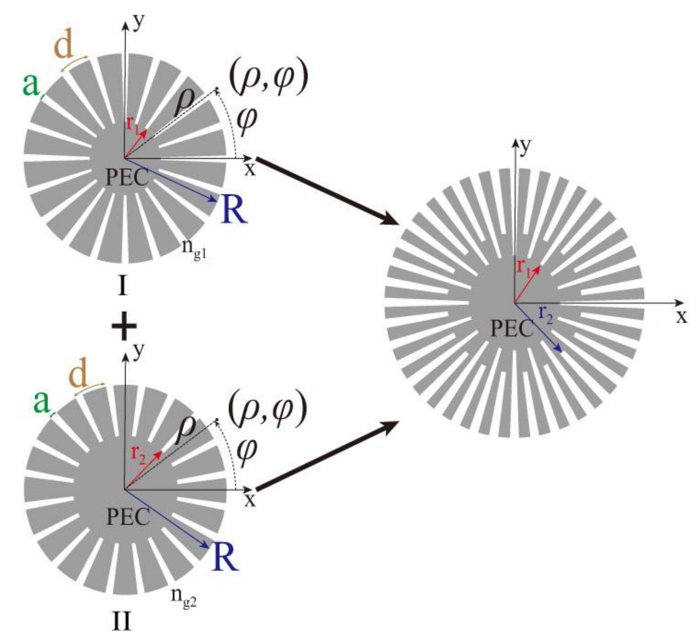

Transmission of slot waveguides with stub + resonators

Double EIT: Four-level atomic system

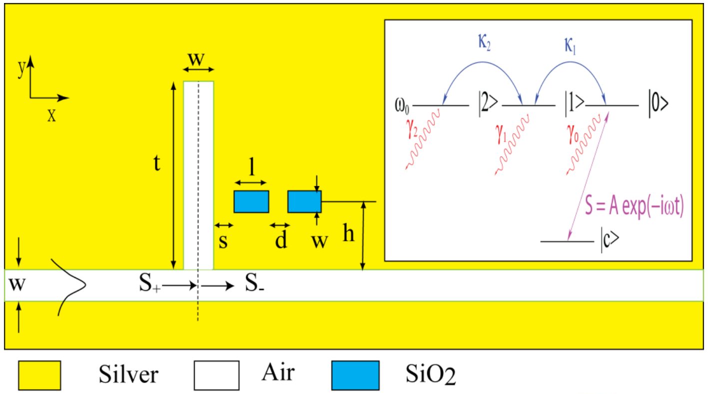

$$\frac{da_0}{dt} = (j\omega_0 - \gamma_0 - \gamma_e)a_0 + e^{j\theta}\sqrt{\gamma_e}S_+ - j\kappa_1 a_1$$

$$\frac{da_1}{dt} = (j\omega_1 - \gamma_1)a_1 - j\kappa_1 a_0 - j\kappa_2 a_2$$

$$\frac{da_2}{dt} = (j\omega_2 - \gamma_2)a_2 - j\kappa_2 a_1$$

$$S_- = S_+ - e^{-j\theta}\sqrt{\gamma_e}a_0$$

$$t = \frac{S_-}{S_+}$$

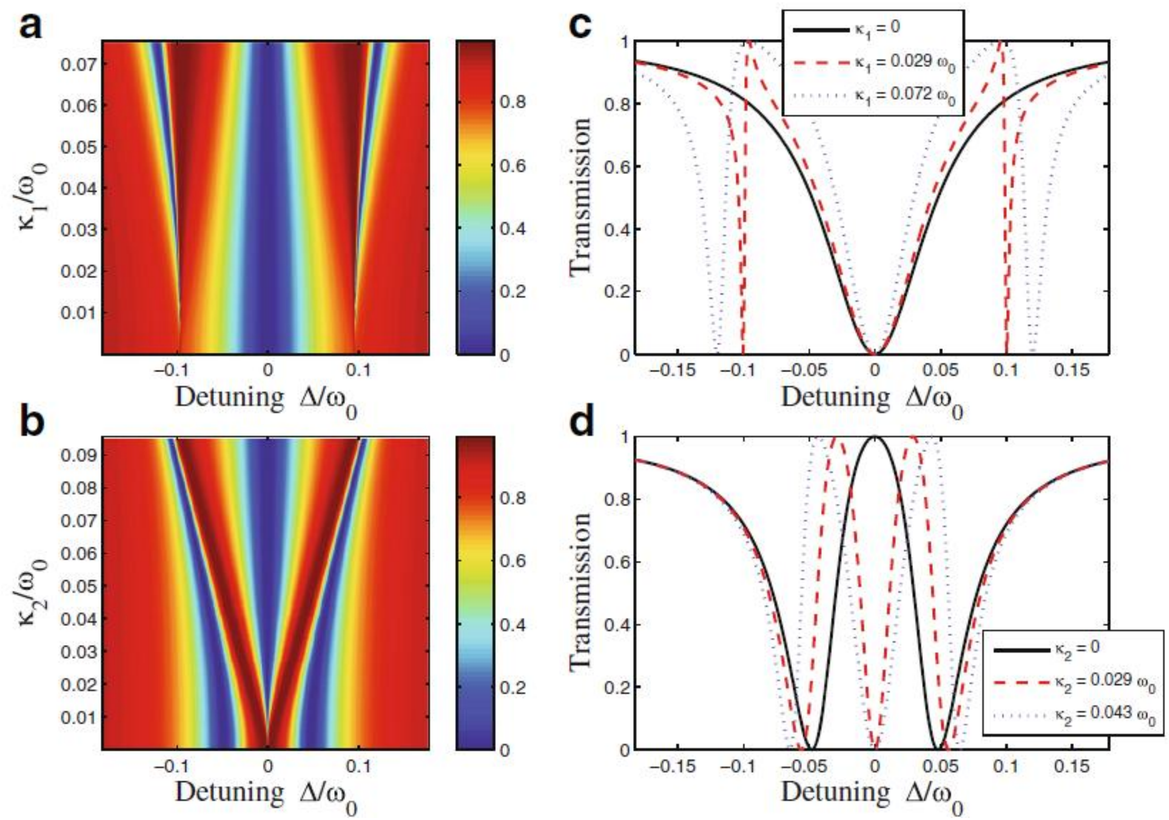

Z. Liu et al., Plamonics 10, 1057 (2015)

Coherent plasmonic wave interference

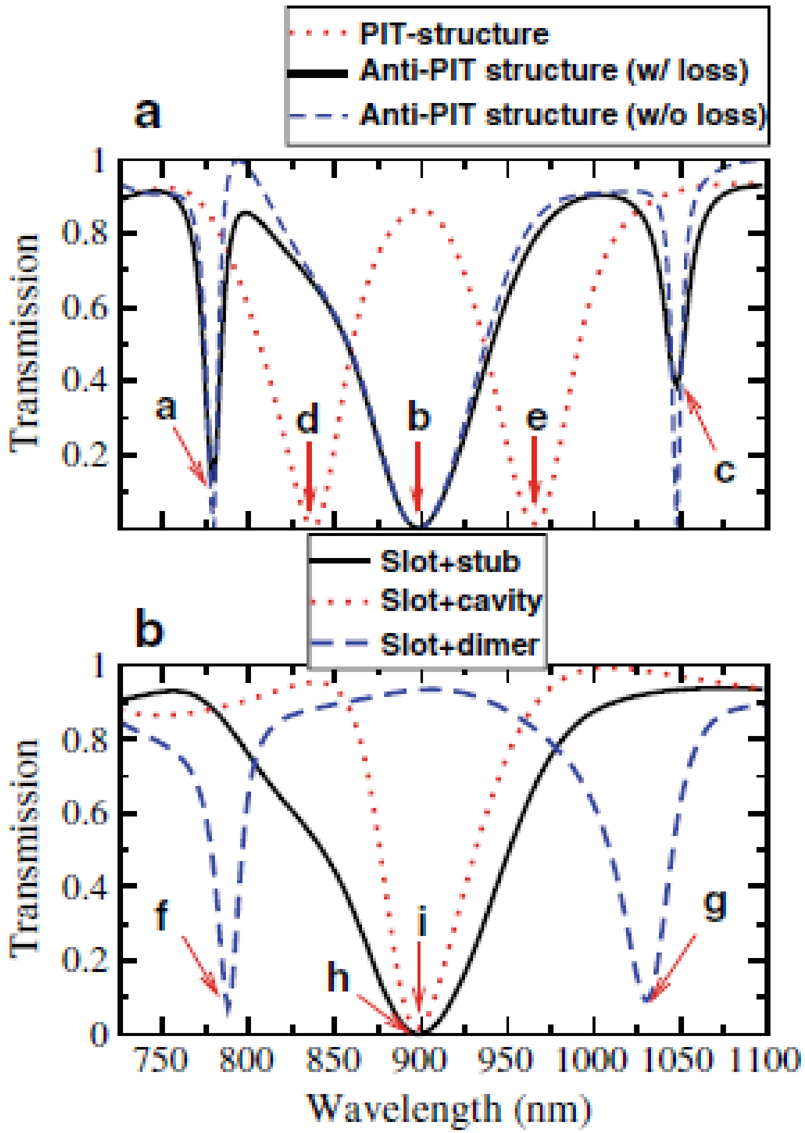

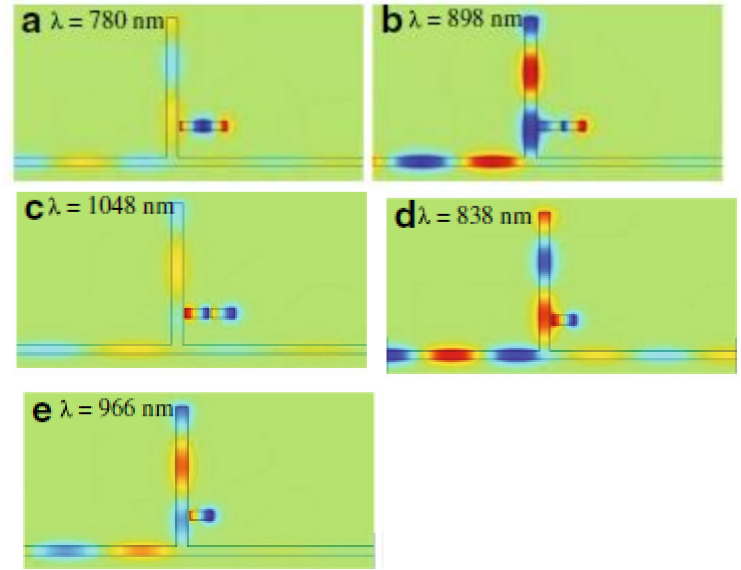

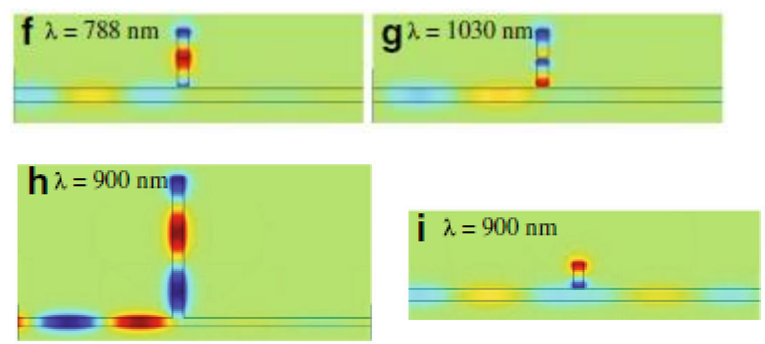

CMT vs. FEM

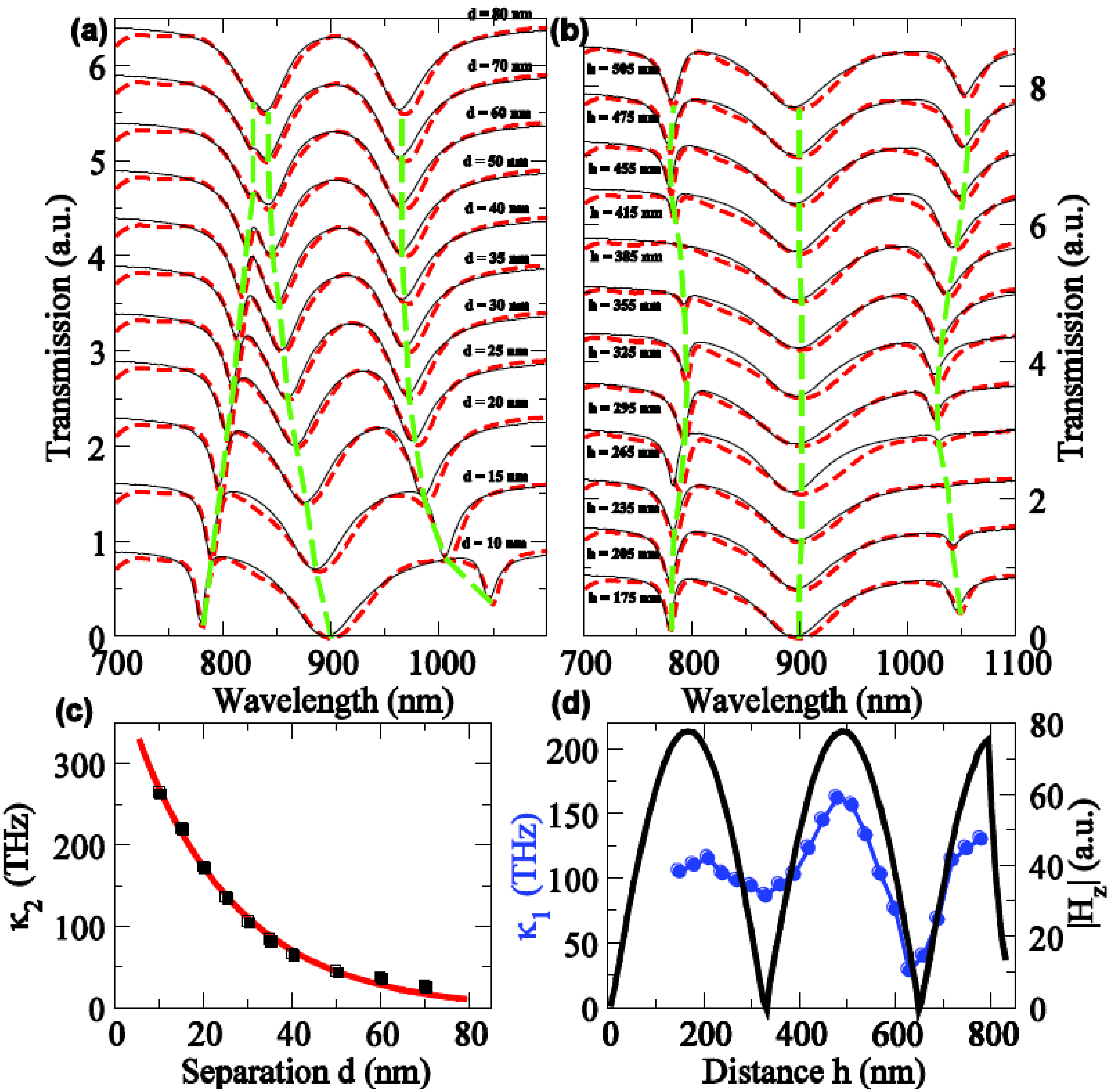

$$T = \left|\frac{S_-}{S_+}\right|^2 = \left|1 - \frac{\gamma_e}{j(\omega-\omega_0)+\gamma_0+\gamma_e+A}\right|^2$$

$$A = \kappa_1^2 / [\, j(\omega-\omega_1)+\gamma_1+B]$$

$$B = \kappa_2^2 / [\, j(\omega-\omega_2)+\gamma_2]$$

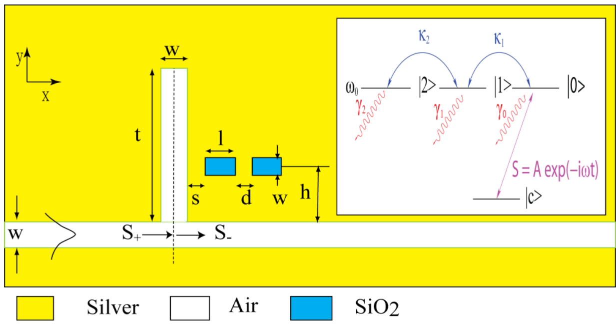

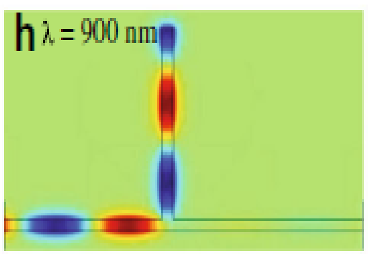

EIT by interactions between Bragg gap and 'polariton' gap

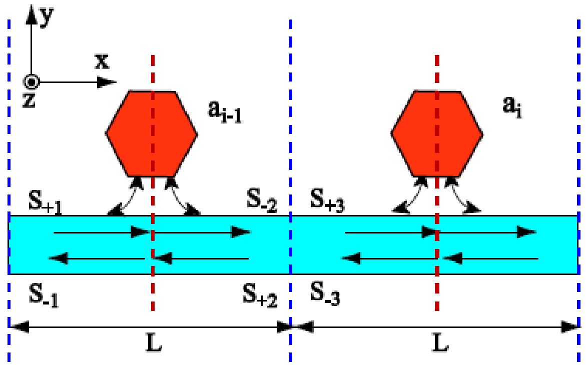

Coupled mode theory

$$\mathbf{a}_i = \left(a_i^1 \quad a_i^2 \quad \cdots \quad a_i^m\right)^T$$

$$\frac{d\mathbf{a}_i}{dt} = \left(-i\mathbf{\Omega} - \mathbf{\Xi}_0 - \mathbf{\Xi}_e\right)\mathbf{a}_i + \mathbf{\Gamma}^T\mathbf{S}_+$$

$$\mathbf{S}_- = \mathbf{C}_i\mathbf{S}_+ + \mathbf{B}_i\mathbf{a}_i$$

$$\begin{pmatrix} S_{-2} \\ S_{+2} \end{pmatrix} = \frac{1}{t}\begin{pmatrix} t^2 - r^2 & r \\ -r & 1 \end{pmatrix}\begin{pmatrix} S_{+1} \\ S_{-1} \end{pmatrix} = \mathbf{M}_1\begin{pmatrix} S_{+1} \\ S_{-1} \end{pmatrix}$$

$$\begin{pmatrix} S_{+3} \\ S_{-3} \end{pmatrix} = \begin{pmatrix} \exp(i\delta) & 0 \\ 0 & \exp(-i\delta) \end{pmatrix}\begin{pmatrix} S_{-2} \\ S_{+2} \end{pmatrix} = \mathbf{M}_2\begin{pmatrix} S_{-2} \\ S_{+2} \end{pmatrix}$$

$$\mathbf{M} = (\mathbf{M}_2\mathbf{M}_1)^n$$

Transmission: $T = \left|1/M_{22}\right|^2$

Dispersion: $\det\left|\mathbf{M} - \mathbf{I}e^{iK_BL}\right| = 0$

$$r = \frac{S_{-1}}{S_{+1}} = \frac{-\gamma_e}{i(\omega_1 - \omega) + \gamma_e}, \quad t = \frac{S_{-2}}{S_{+1}} = \frac{i(\omega_1 - \omega)}{i(\omega_1 - \omega) + \gamma_e}$$

Single resonances case

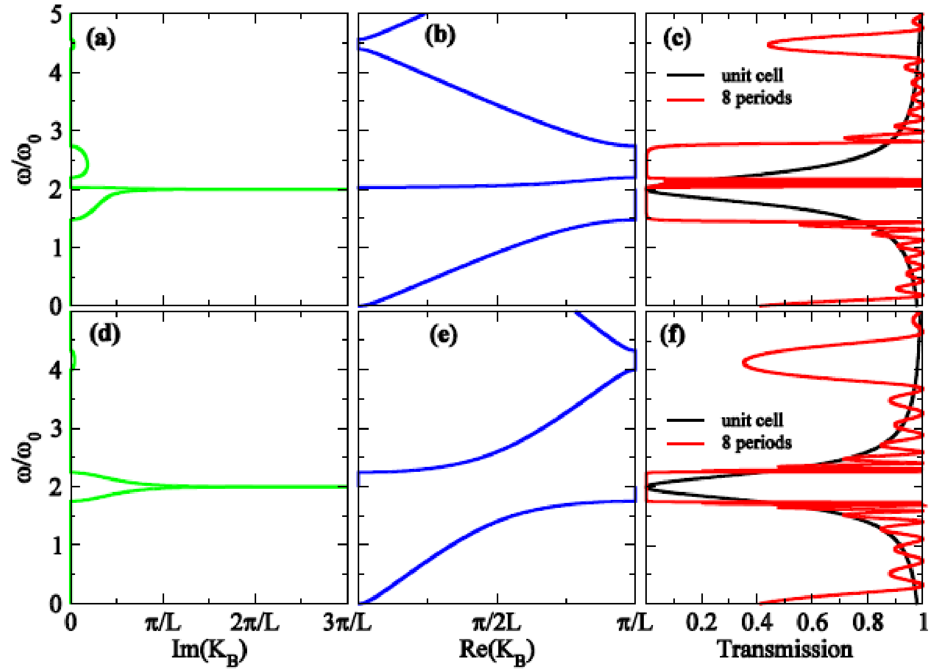

Z. Liu et al., J. Opt. 18, 015005 (2016)

Two-resonances case

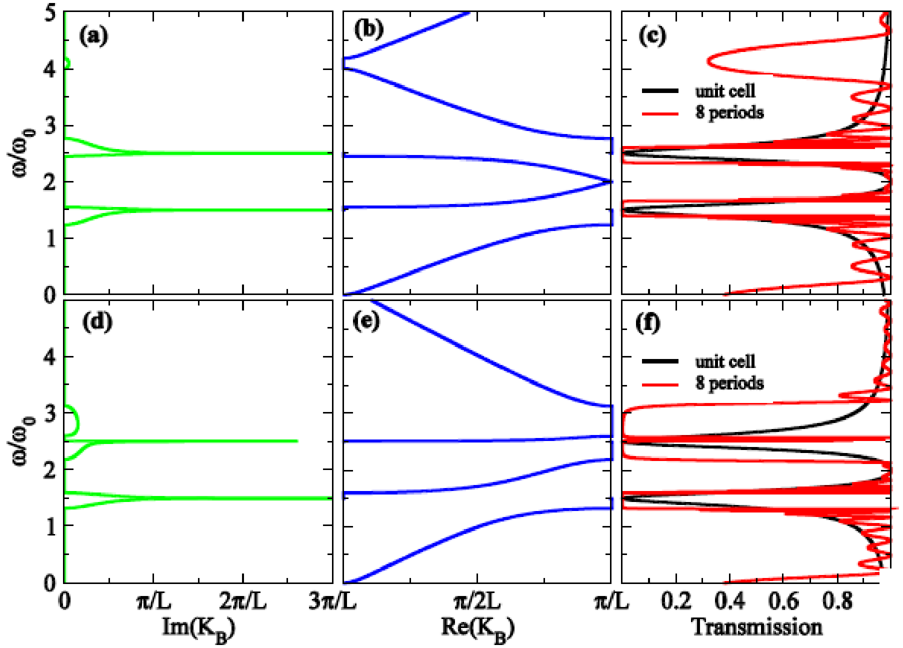

$$t=\frac{S_{-2}}{S_{+1}}=1+\frac{-\gamma_e}{i\left(\omega_0-\omega\right)+\gamma_e+\dfrac{\mu^2}{i\left(\omega_1-\omega\right)}}.$$

$$r=\frac{S_{-1}}{S_{+1}}=\frac{-\gamma_e}{i\left(\omega_0-\omega\right)+\gamma_e+\dfrac{\mu^2}{i\left(\omega_1-\omega\right)}},$$

Three-resonances case

$$t=\frac{S_{-2}}{S_{+1}}=1+\frac{-\gamma_e}{i\left(\omega_0-\omega\right)+\gamma_e+\dfrac{\mu_1^2}{i\left(\omega_1-\omega\right)+\dfrac{\mu_2^2}{i\left(\omega_2-\omega\right)}}},$$

$$r=\frac{S_{-1}}{S_{+1}}=\frac{-\gamma_e}{i\left(\omega_0-\omega\right)+\gamma_e+\dfrac{\mu_1^2}{i\left(\omega_1-\omega\right)+\dfrac{\mu_2^2}{i\left(\omega_2-\omega\right)}}}.$$

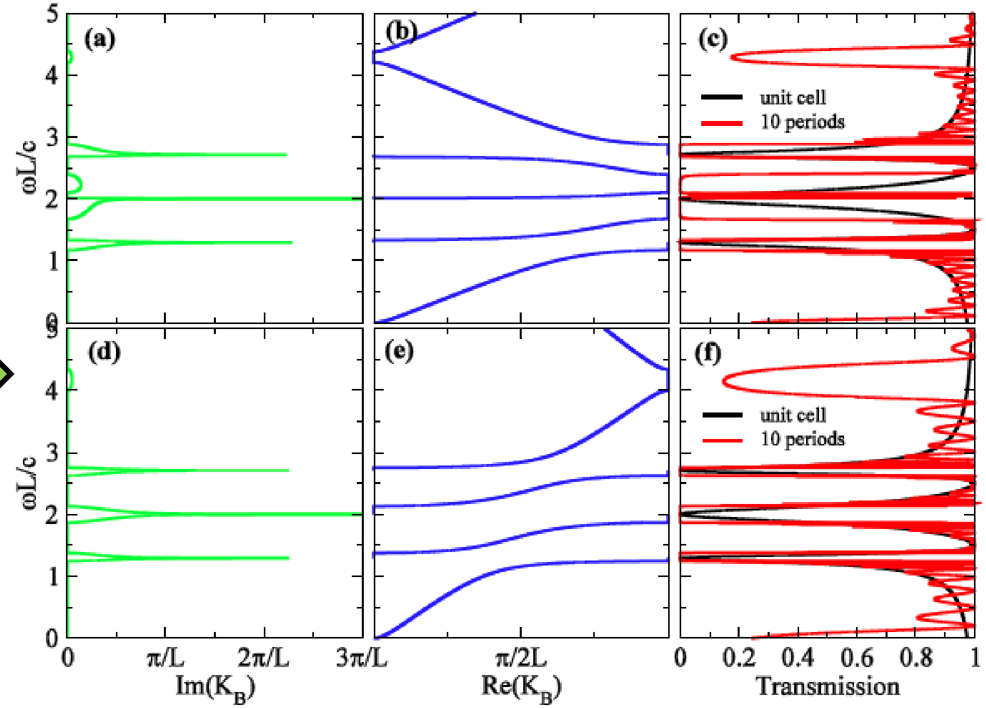

Plasmonic slot waveguide realization

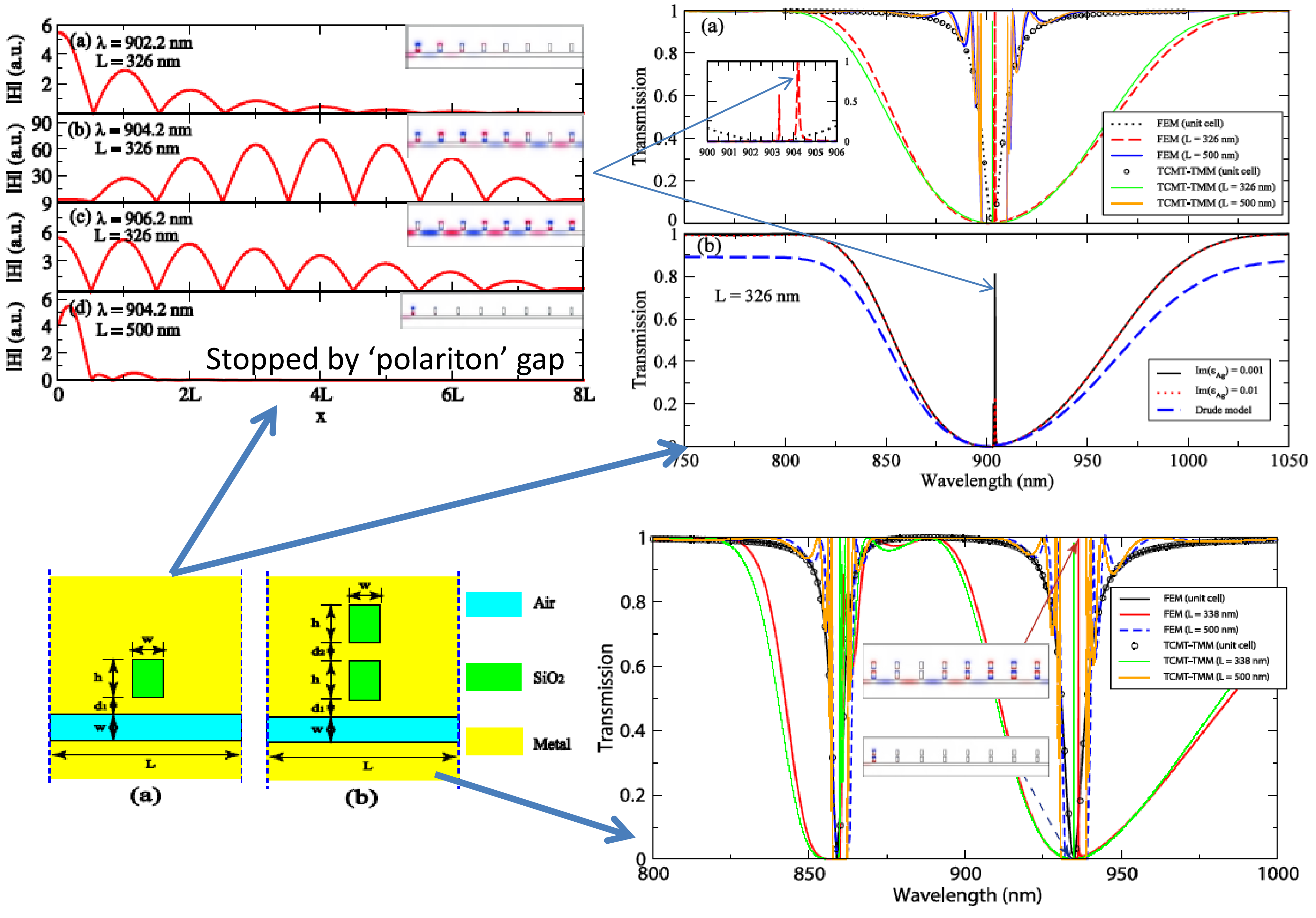

II. Toroidal resonance and its interactions with other modes

Magnetic and toroidal cavity modes

Metal-Dielectric-Metal

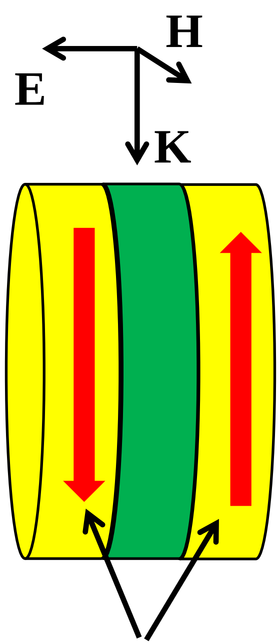

anti-parallel going currents

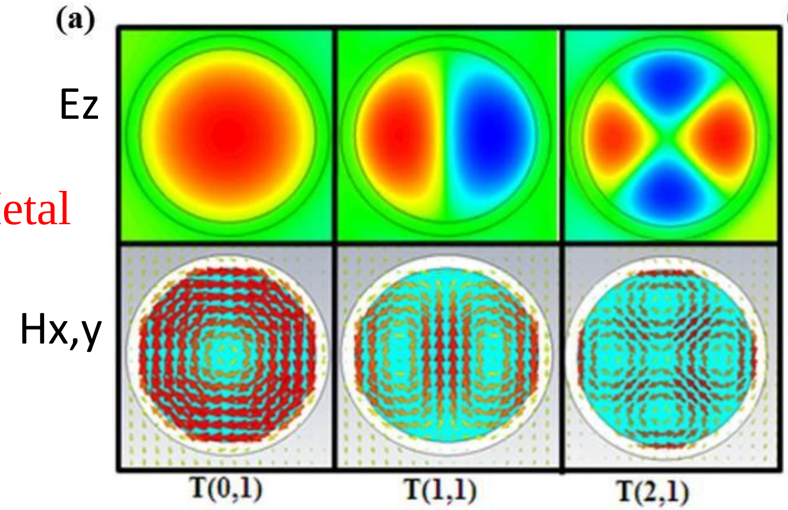

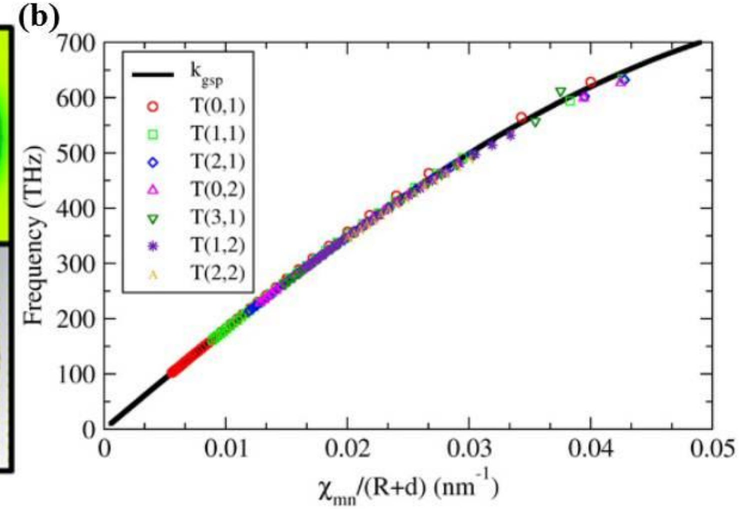

$$E_z(\rho, \phi, z) = a(z)[H_m^{(1)}(k_{gsp}\rho) + r_m H_m^{(2)}(k_{gsp}\rho)]e^{im\phi}$$

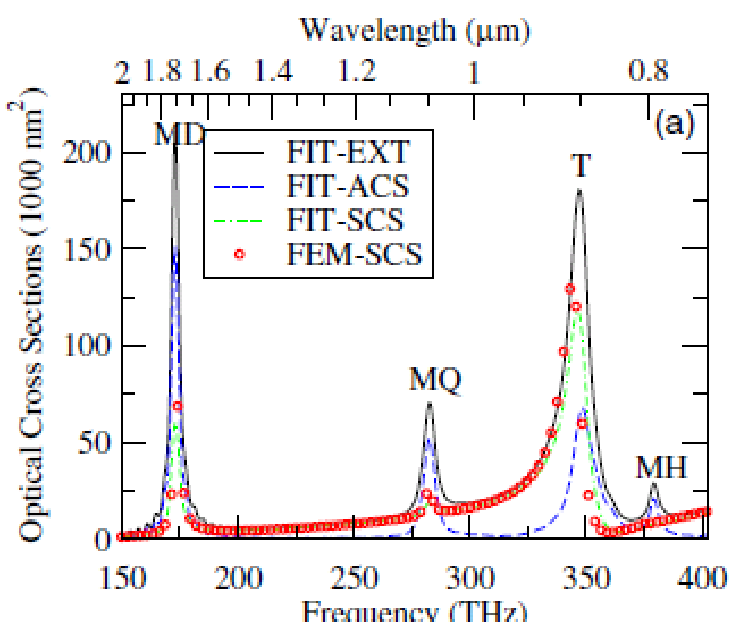

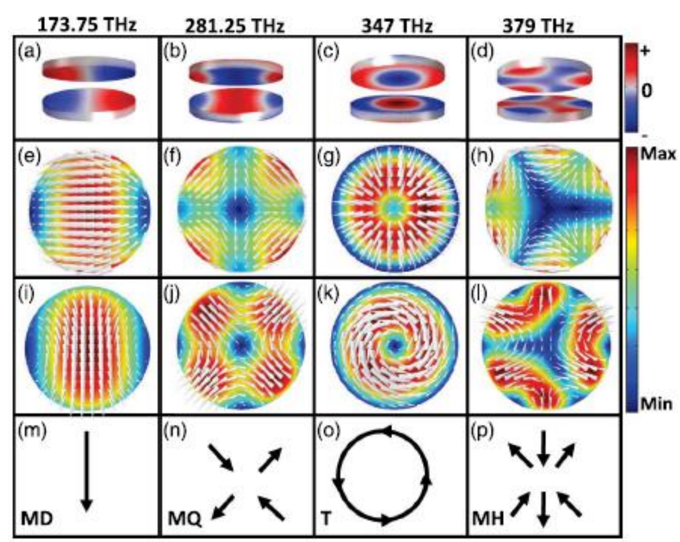

Q. Zhang et at., ACS Photonics 2, 60 (2015)
Q. Zhang et al., J. Opt. Soc. Am. B 5, 1103 (2014)

EIT and Fano resonance induced by coupling between antenna mode and cavity modes

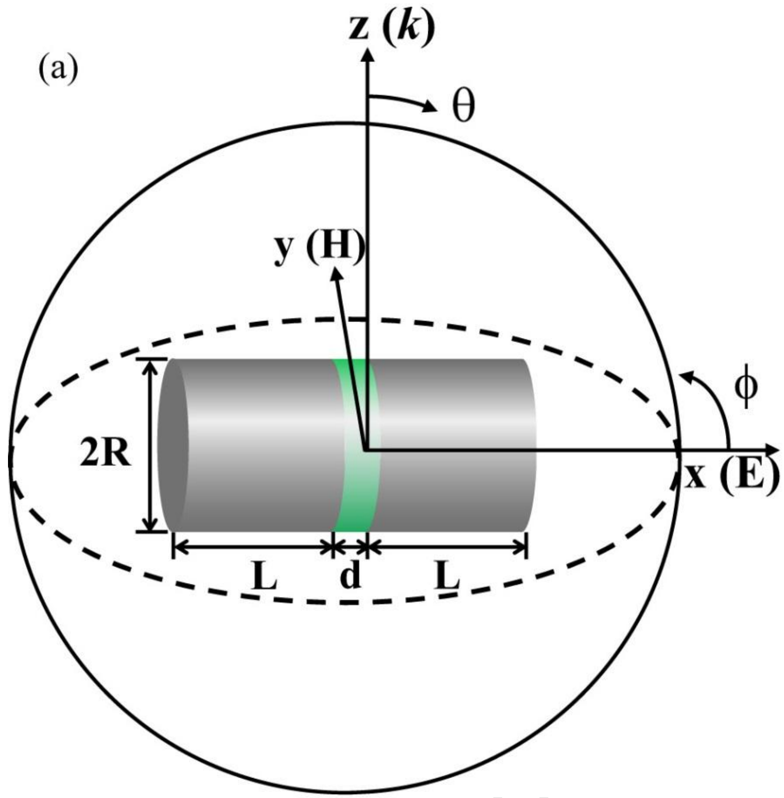

$$L = 90\ nm,\ R = 50\ nm, and\ d = 20\ nm$$

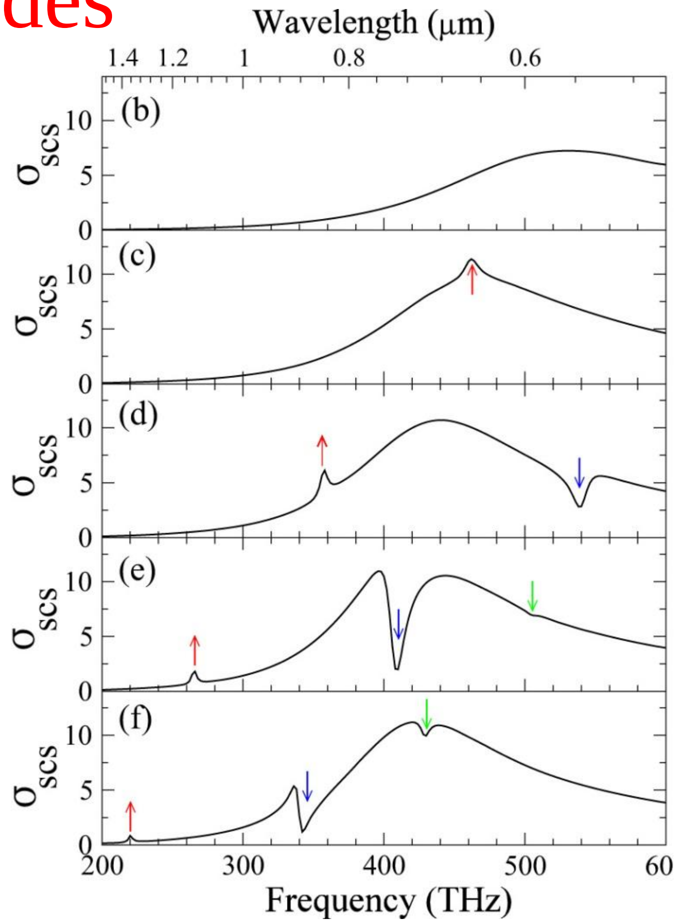

$\varepsilon_{load} = 1$

$\varepsilon_{load} = 3$

$\varepsilon_{load} = 6$

$\varepsilon_{load} = 12$

$\varepsilon_{load} = 18$

Delicately designed dipole antenna
Metal: Ag ------ **antenna mode**
Dielectric: ε_{load} ------ **cavity mode**
(different angular momentum)

Envelope: broad dipole resonance

sub-peak **first dip** **second dip**

Q. Zhang et al., Sci. Rep. 5, 17234 (2015)

Multipole decomposition in spherical basis

$$a_{lm}=\frac{(-i)^{l+1}kr}{h_l^{(1)}(kr)E_0\left[\pi(2l+1)l(l+1)\right]^{\frac{1}{2}}}\int_0^{2\pi}\int_0^{\pi}Y_{lm}^*(\theta,\phi)\hat{\mathbf{r}}\cdot\mathbf{E}_s(\mathbf{r})\sin(\theta)d\theta d\phi$$

$$b_{lm}=\frac{(-i)^{l}\eta kr}{h_l^{(1)}(kr)E_0\left[\pi(2l+1)l(l+1)\right]^{\frac{1}{2}}}\int_0^{2\pi}\int_0^{\pi}Y_{lm}^*(\theta,\phi)\hat{\mathbf{r}}\cdot\mathbf{H}_s(\mathbf{r})\sin(\theta)d\theta d\phi$$

$h_l^{(1)} \rightarrow$ spherical Hankel function

$Y_{lm}(\theta,\phi) \rightarrow$ Spherical Harmonics

$$C_s=\frac{\pi}{k^2}\sum_{l=1}^{\infty}\sum_{m=-l}^{l}(2l+1)\left[\left|a_{lm}\right|^2+\left|b_{lm}\right|^2\right]$$

η wave impendence in background

$$a_{\mathrm{E}}(l,m)=\frac{(-\mathrm{i})^{l-1}k^2\eta O_{lm}}{E_0[\pi(2l+1)]^{1/2}}\int\exp(-\mathrm{i}m\phi)\Big\{\left[\Psi_l(kr)+\Psi_l''(kr)\right]P_l^m(\cos\theta)\hat{\boldsymbol{r}}\cdot\boldsymbol{J}_{\mathrm{S},j}(\boldsymbol{r})$$
$$+\frac{\Psi_l'(kr)}{kr}\left[\tau_{lm}(\theta)\hat{\theta}\cdot\boldsymbol{J}_{\mathrm{S},j}(\boldsymbol{r})-\mathrm{i}\pi_{lm}(\theta)\hat{\phi}\cdot\boldsymbol{J}_{\mathrm{S},j}(\boldsymbol{r})\right]\Big\}\mathrm{d}^3r,$$

$$a_{\mathrm{M}}(l,m)=\frac{(-\mathrm{i})^{l+1}k^2\eta O_{lm}}{E_0[\pi(2l+1)]^{1/2}}\int\exp(-\mathrm{i}m\phi)j_l(kr)\left[\mathrm{i}\pi_{lm}(\theta)\hat{\theta}\cdot\boldsymbol{J}_{\mathrm{S},j}(\boldsymbol{r})+\tau_{lm}(\theta)\hat{\phi}\cdot\boldsymbol{J}_{\mathrm{S},j}(\boldsymbol{r})\right]\mathrm{d}^3r$$

$$O_{lm}=\frac{1}{[l(l+1)]^{1/2}}\left[\frac{2l+1}{4\pi}\frac{(l-m)!}{(l+m)!}\right]^{1/2},$$

$$\tau_{lm}(\theta)=\frac{\mathrm{d}}{\mathrm{d}\theta}P_l^m(\cos\theta),$$

$$\pi_{lm}(\theta)=\frac{m}{\sin\theta}P_l^m(\cos\theta).$$

Multipole decomposition in Cartesian basis

$$I = \left(\frac{2\omega^4}{3c^3}|\mathbf{P}|^2 + \frac{2\omega^4}{3c^3}|\mathbf{M}|^2 + \frac{4\omega^5}{3c^4}\mathrm{Im}(\mathbf{P}\cdot\mathbf{T}^*) + \frac{2\omega^6}{3c^5}|\mathbf{T}|^2 + \frac{\omega^6}{20c^5}\left|\mathbf{Q}^e\right|^2 + \frac{\omega^6}{20c^5}\left|\mathbf{Q}^m\right|^2 - \frac{2\omega^6}{15c^5}\mathrm{Re}\left(\mathbf{M}^*\left\langle \mathbf{R}_\mathbf{m}^\mathbf{2}\right\rangle\right)\right)/(8\pi\varepsilon_0)$$

$$P_\alpha = -\frac{1}{i\omega}\int J_\alpha d^3 r$$

$$M_\alpha = \frac{1}{2c}\int [\mathbf{r}\times\mathbf{J}]_\alpha d^3 r$$

$$T_\alpha = \frac{1}{10c}\int \left[(\mathbf{r}\cdot\mathbf{J})r_\alpha - 2r^2 J_\alpha\right] d^3 r$$

$$Q^e_{\alpha\beta} = -\frac{1}{i\omega}\int\left[r_\alpha J_\beta + J_\alpha r_\beta - \frac{2}{3}\delta_{\alpha\beta}(\mathbf{r}\cdot\mathbf{J})\right] d^3 r$$

$$Q^m_{\alpha\beta} = \frac{1}{3c}\int\left[[\mathbf{r}\times\mathbf{J}]_\alpha r_\beta + r_\alpha [\mathbf{r}\times\mathbf{J}]_\beta\right] d^3 r$$

$$\left\langle R_m^2\right\rangle_\alpha = \frac{1}{2c}\int d^3 r [\mathbf{r}\times\mathbf{J}]_\alpha r^2$$

Note :
The SI form is just obtained by multiplying **I** in CGS form by $\frac{1}{4\pi\varepsilon_0}$

$$C_{SCS} = \frac{2Z_0 \mathrm{I}}{|E_0|^2}$$

$$E = \frac{k^2}{4\pi\varepsilon_0}\frac{e^{ikr}}{r}\left\{\hat{\mathbf{n}}\times(\mathbf{P}\times\hat{\mathbf{n}}) + (\mathbf{M}\times\hat{\mathbf{n}}) + ik\cdot\hat{\mathbf{n}}\times(\mathbf{T}\times\hat{\mathbf{n}}) + \frac{ik}{2}\hat{\mathbf{n}}\times[\hat{\mathbf{n}}\times(\mathbf{Q}^e\cdot\hat{\mathbf{n}})] + \frac{ik}{2}\hat{\mathbf{n}}\times(\mathbf{Q}^m\cdot\hat{\mathbf{n}})\right\}$$

Multipole scattering decomposition: benchmark

R = 65 **nm**

$\varepsilon = 22$

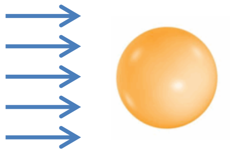

High dielectric sphere benchmark

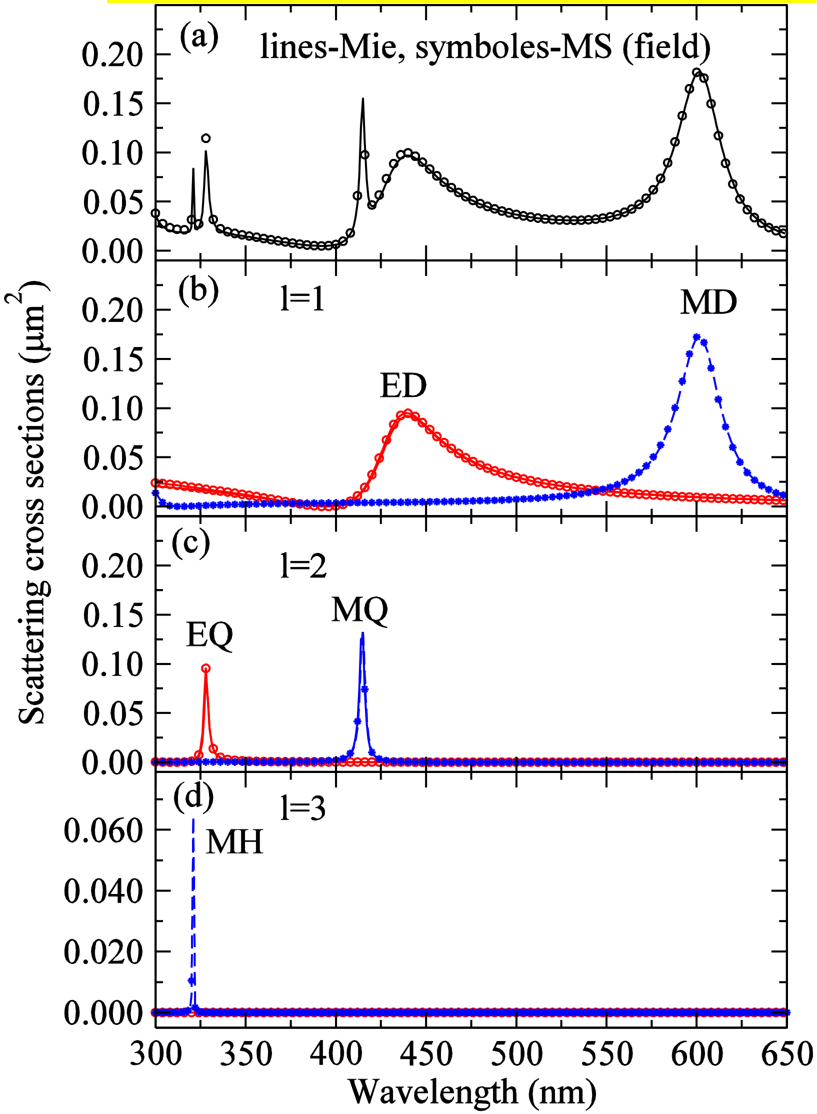

Numerical vs. Mie theory

ED:	**electric dipole**	a_1
MD:	**magnetic dipole**	b_1
EQ:	**electric quadrupole**	a_2
MQ:	**magnetic quadrupole**	b_2
MH:	**magnetic hexapole**	b_3

Multipole scattering decomposition: Application

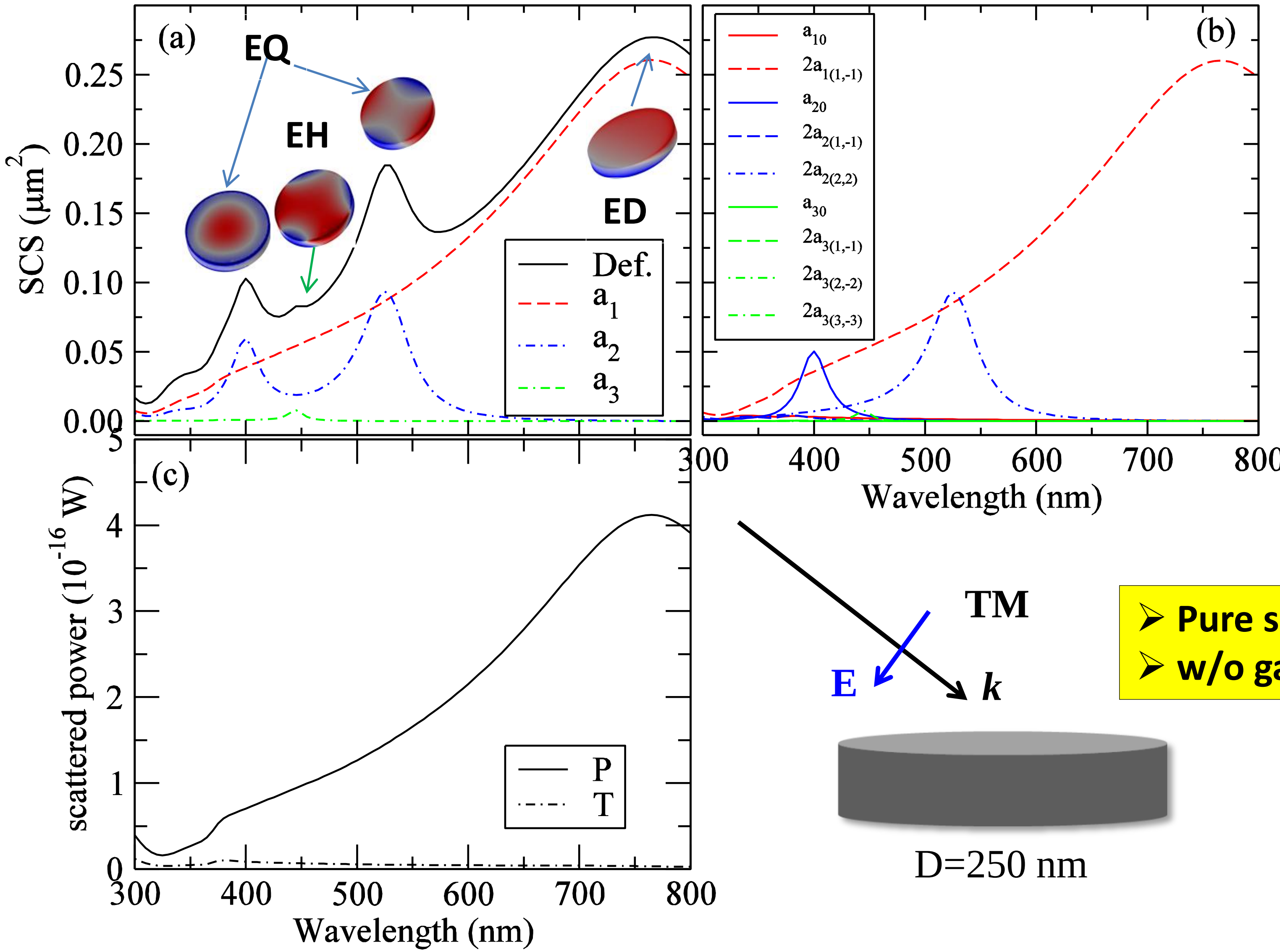

- Pure silver disk
- w/o gap layer

Coexistence of scattering suppression and enhancement

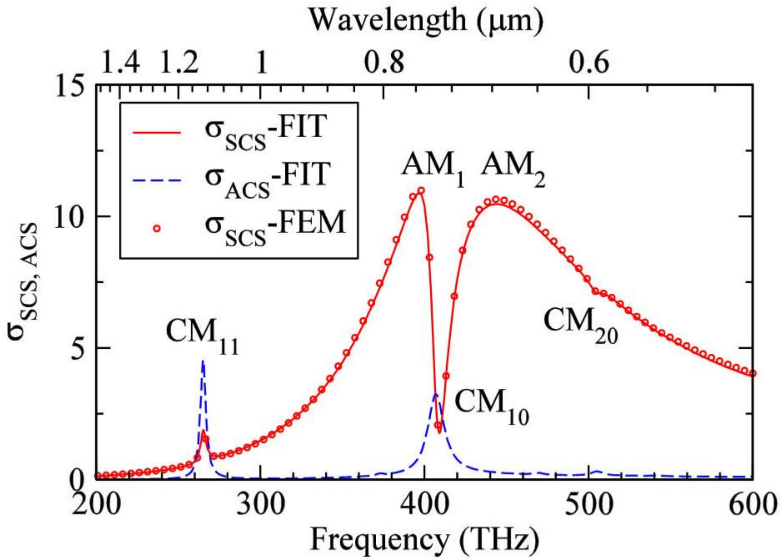

Two families of resonances: AM and CMs

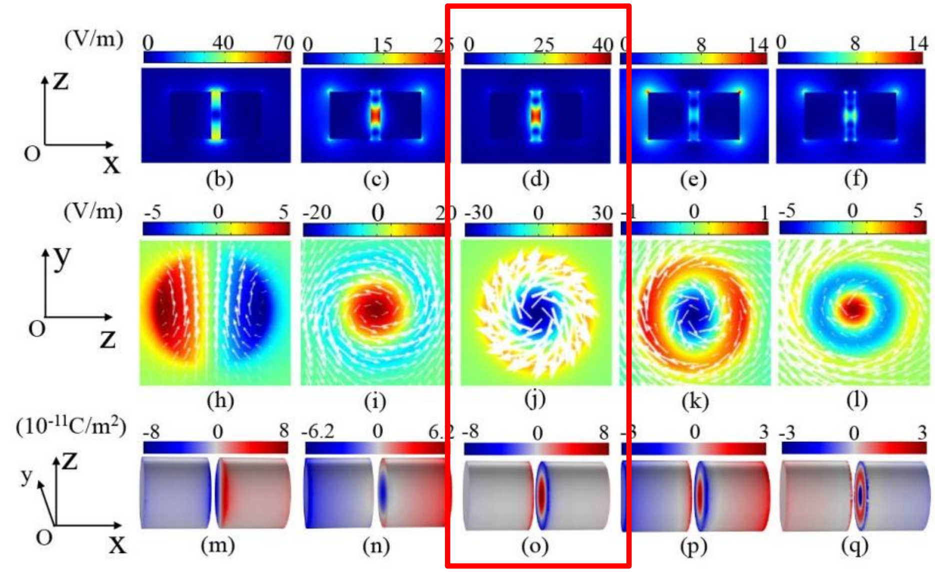

Dipole-toroidal Fano resonance suppresses the bright *electric antenna mode*

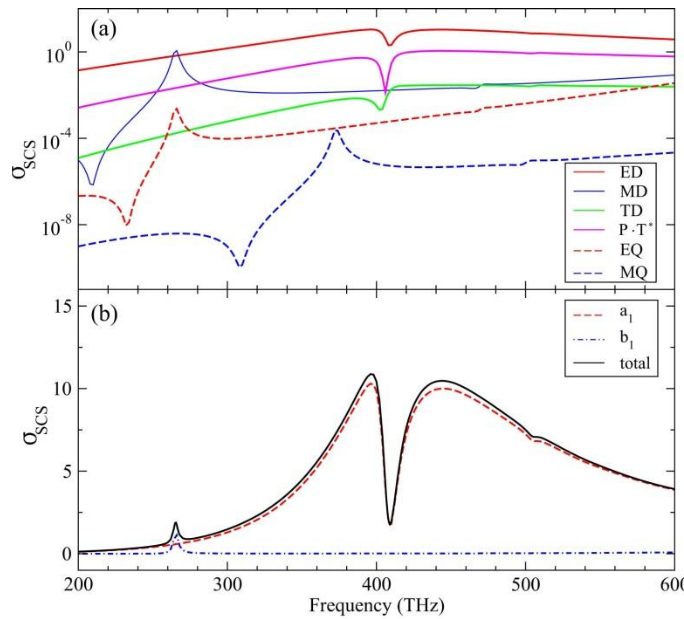

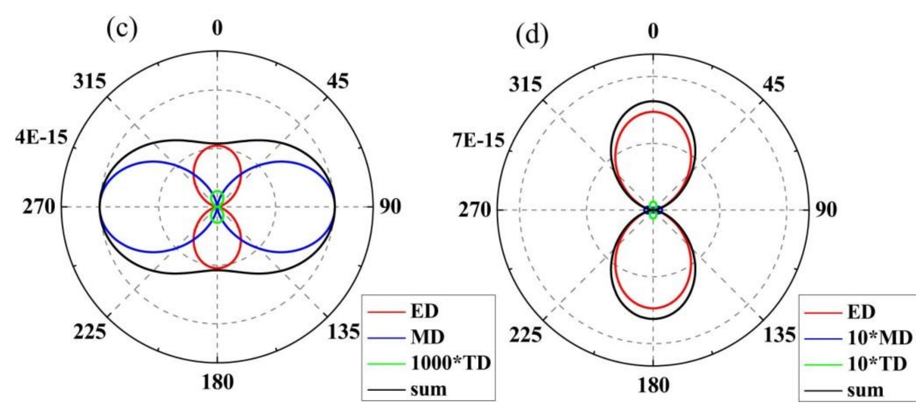

Different far field scattering patterns

Spin-dependent emission control

Moments identified by multipole decomposition

Coupled oscillator model: bright + sub-bright + dark modes

$$\begin{pmatrix} \chi_p \\ \chi_m \\ \chi_t \end{pmatrix} = \begin{pmatrix} \omega_p^2 - \omega^2 + i\gamma_p\omega & 0 & \kappa^2 \\ 0 & \omega_m^2 - \omega^2 + i\gamma_m\omega & 0 \\ \kappa^2 & 0 & \omega_t^2 - \omega^2 + i\gamma_t\omega \end{pmatrix}^{-1} \cdot \begin{pmatrix} G_p \\ G_m \\ 0 \end{pmatrix}$$

$$E_z(\rho,\phi,z) \sim AF(z)G(\rho)$$

$$E_z(\rho,\phi,z) = a(z)f(k_{gsp}\rho)e^{im\phi}$$

$$\int_0^{2\pi} e^{i(m-m')\phi}d\phi = 2\pi\delta(m-m')$$

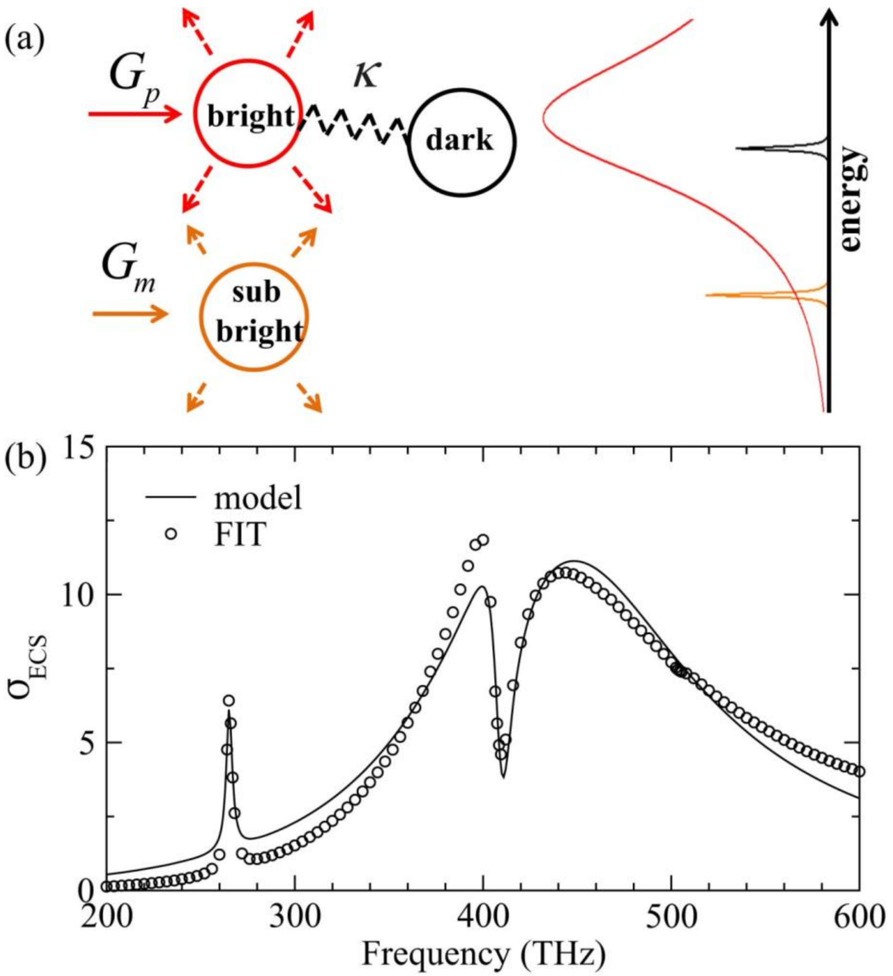

Tunable by geometry and loaded material

L = 90 nm, d = 20 nm

$\varepsilon = 12$, d = 20 nm

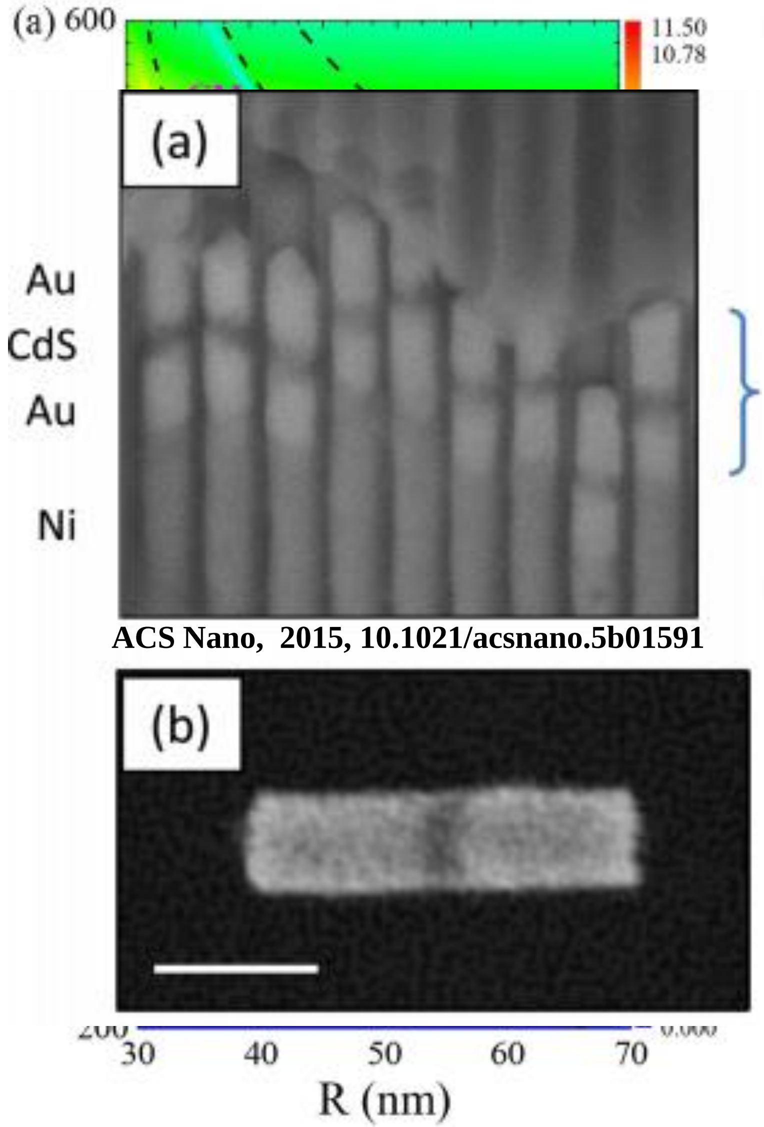

ACS Nano, 2015, 10.1021/acsnano.5b01591

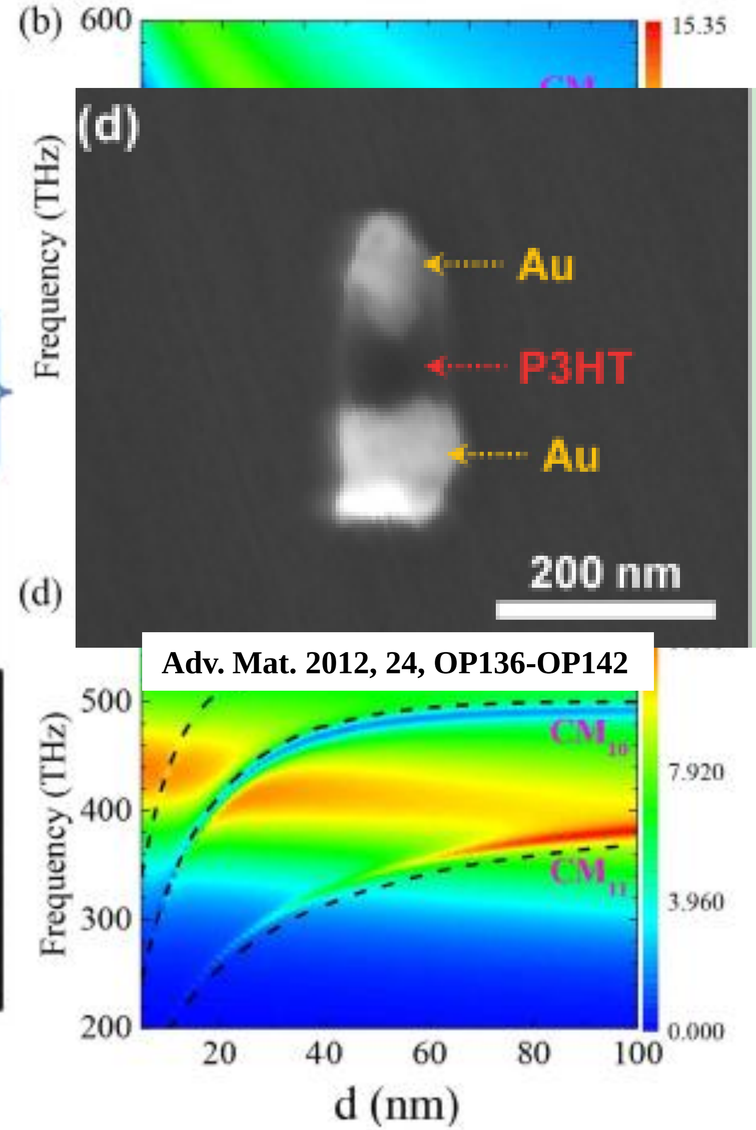

Adv. Mat. 2012, 24, OP136-OP142

III. Absence of Exceptional Points in Coupled Waveguides

PT-symmetry and mode coalescence in 2D coupler

In optics

$$\boxed{n(r) = n^*(-r)}$$

balanced gain/loss contrast

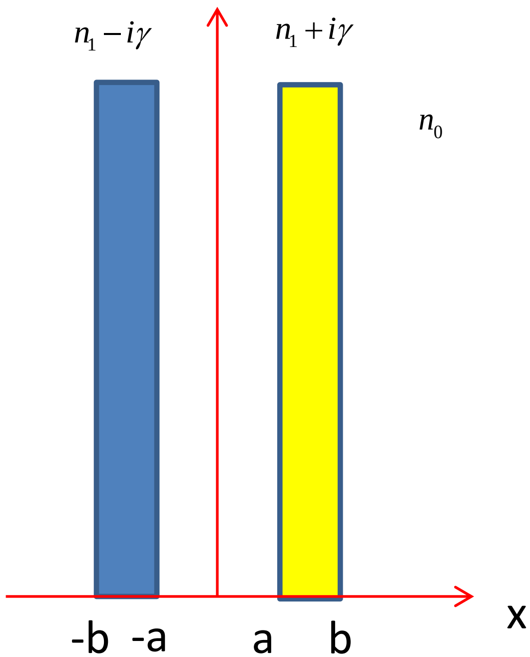

Non-Hermitian Hamiltonian

$$\frac{i}{k_0}\frac{d}{dz}\begin{pmatrix} a_1 \\ a_2 \end{pmatrix} = \begin{pmatrix} n_e + i\gamma_1 & \kappa_{12} \\ \kappa_{12} & n_e - i\gamma_1 \end{pmatrix}\begin{pmatrix} a_1 \\ a_2 \end{pmatrix}$$

$$n_{coupled} = n_e \pm \sqrt{\kappa_{12}{}^2 - \gamma_1{}^2}$$

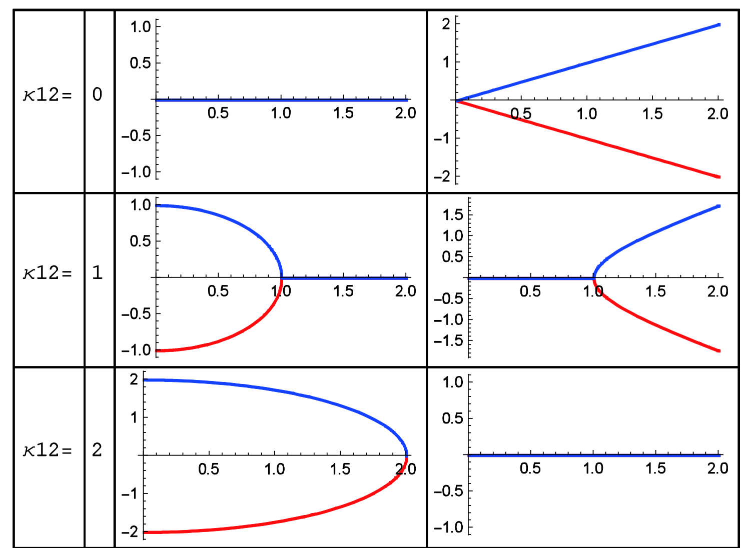

PT-symmetry and EP in 2D waveguide coupler

γ_1

Increasing

Real

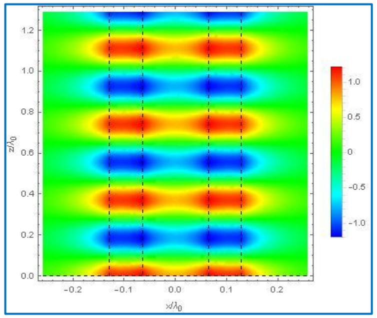

(1, 1)

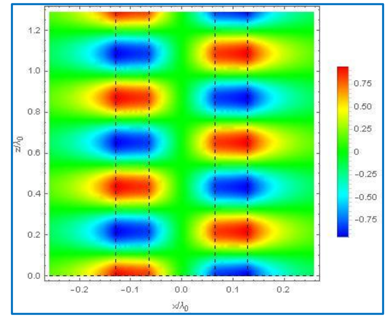

(1, -1)

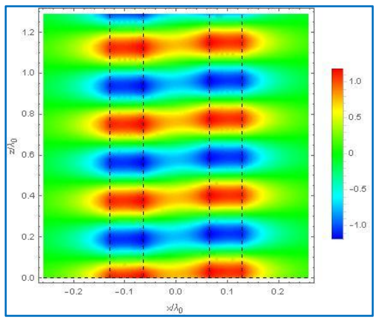

$(1.\ e^{i0.52}\ ,1)$

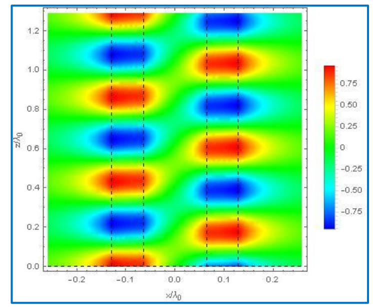

$(1.\ e^{i2.62}\ ,1)$

Exceptional point (EP)

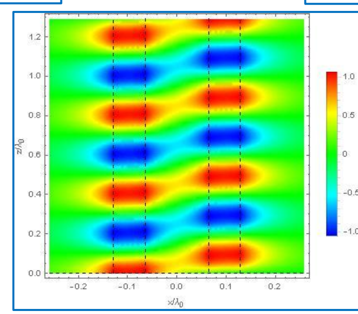

$(1.\ e^{i1.57},1)$

Complex conjugate

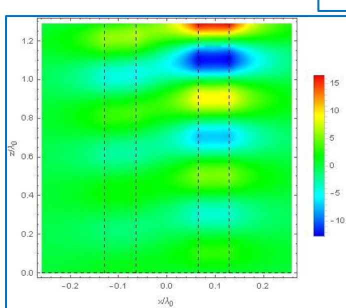

$(2.62\ e^{i1.57},1)$

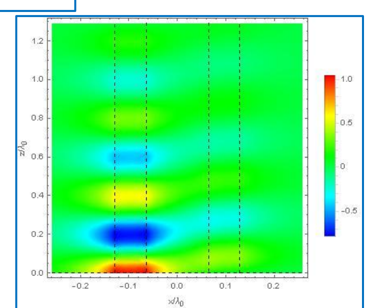

$(0.38\ e^{i1.57},1)$

PT-symmetry in two coupled 3D waveguides

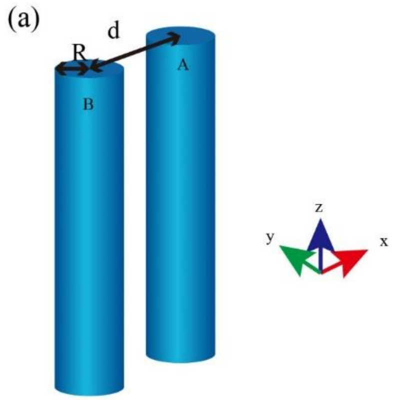

$$n_{A,B} = 3.5 \pm ig$$
$$n_b = 1.5$$
$$R = 0.2\ \mu m$$
$$d = 0.5\ \mu m$$

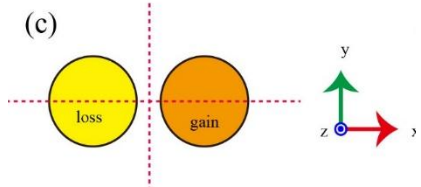

$$\frac{i}{k_0}\frac{d}{dz}\begin{pmatrix} a_1 \\ b_1 \\ a_2 \\ b_2 \end{pmatrix} = \begin{pmatrix} n_e - i\gamma & 0 & \kappa_L & 0 \\ 0 & n_e - i\gamma & 0 & \kappa_T \\ \kappa_L & 0 & n_e + i\gamma & 0 \\ 0 & \kappa_T & 0 & n_e + i\gamma \end{pmatrix}\begin{pmatrix} a_1 \\ b_1 \\ a_2 \\ b_2 \end{pmatrix}$$

$$\frac{i}{k_0}\frac{d}{dz}\begin{pmatrix} a_p \\ b_p \end{pmatrix} = \begin{pmatrix} n_e - i\gamma & \kappa_p \\ \kappa_p & n_e + i\gamma \end{pmatrix}\begin{pmatrix} a_p \\ b_p \end{pmatrix} = H\begin{pmatrix} a_p \\ b_p \end{pmatrix}$$

κ_p: Coupling strength for the longitudinal ($p = L$) and transverse ($p = T$) cases

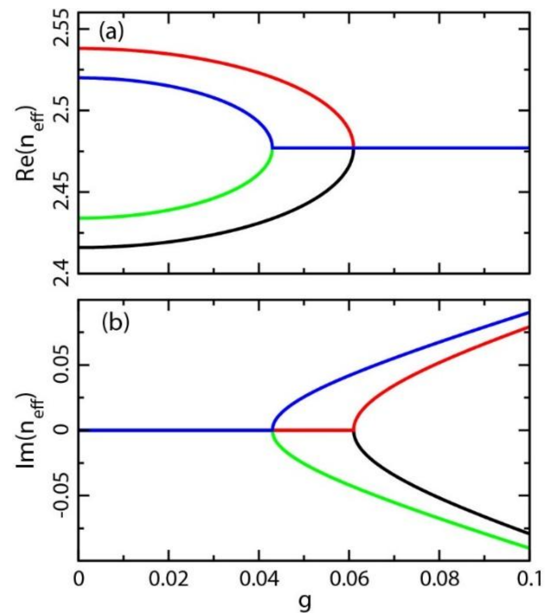

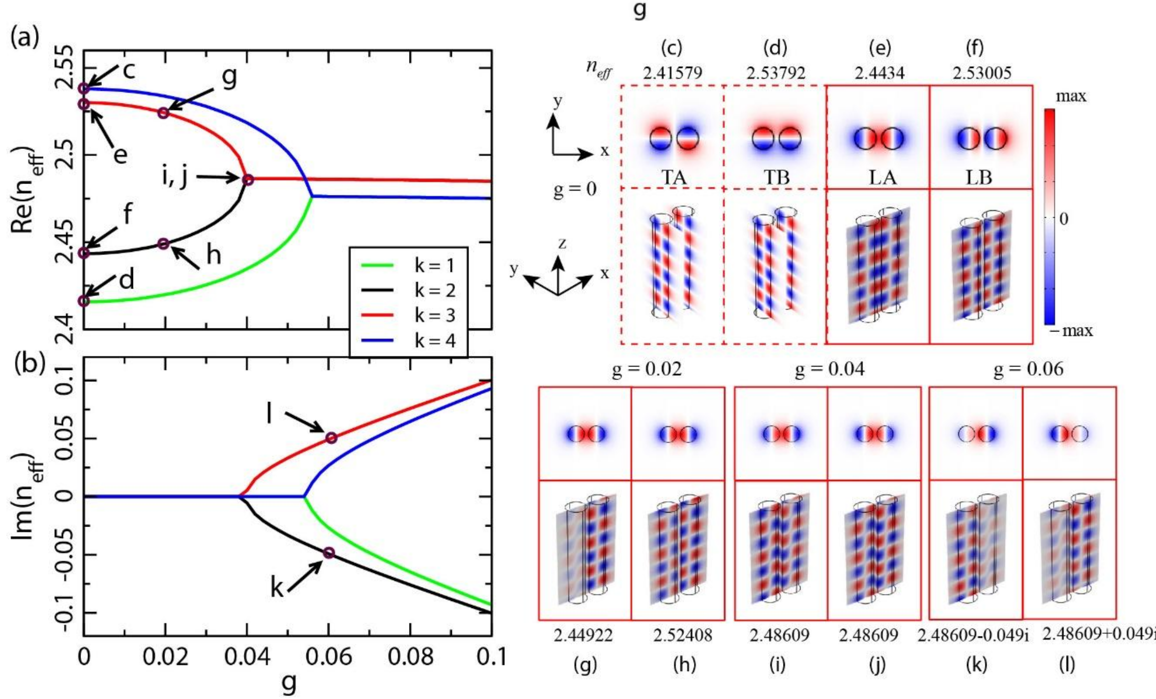

PT-symmetry in four coupled waveguides

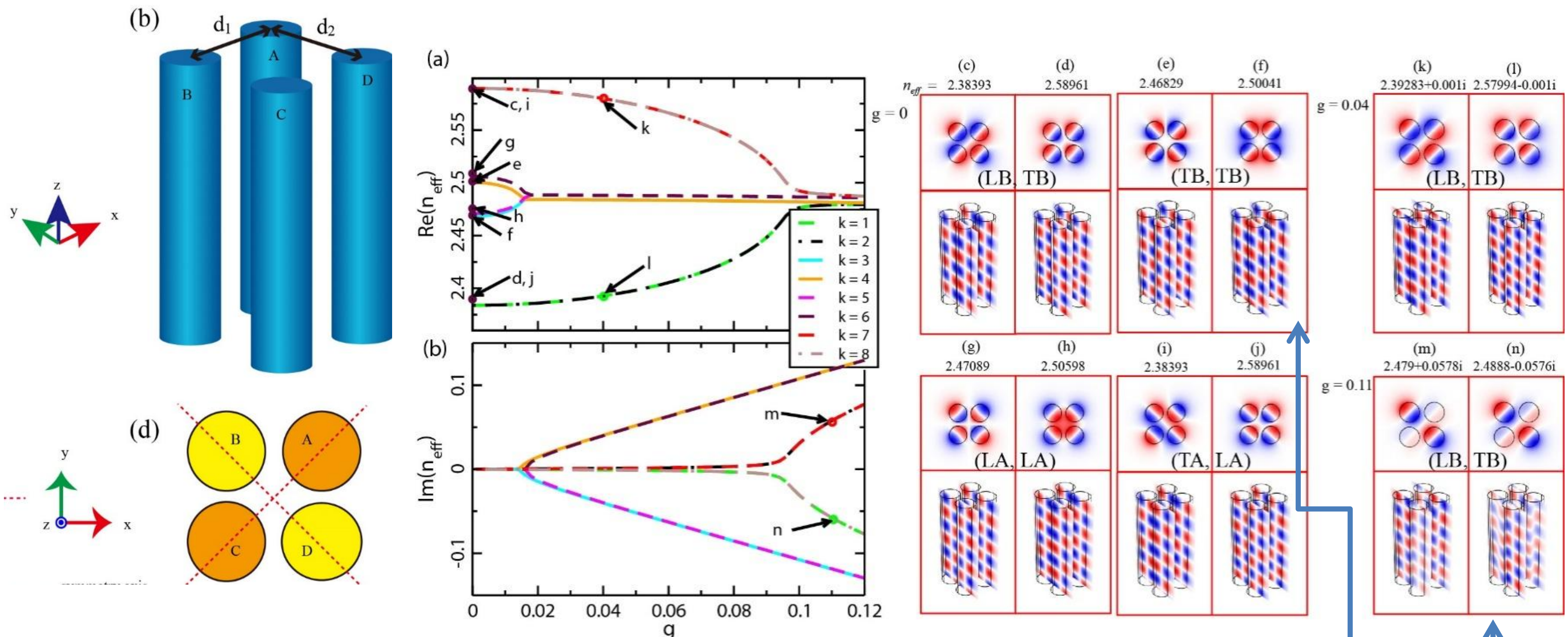

Band 3,4 $$H_1 = \begin{pmatrix} n_e - \kappa_T + i\gamma & K_1 \\ K_1 & n_e - \kappa_T - i\gamma \end{pmatrix}$$ (TB, TB) → With EPs and phase transition

Lattice symmetry
Mode symmetry
PT symmetry

Band 1,7 $$H_2 = \begin{pmatrix} n_e - \kappa_L + i\gamma & K_2 \\ K_2 & n_e - \kappa_T - i\gamma \end{pmatrix}$$ (LB, TB) → **No EPs**
No phase transition

Z. Z. Liu et al., (under review)

Phase rigidity

Ding, Ma, Xiao, Zhang and Chan
arXiv:1509.06886 (2015)

$$\boxed{r_k(\gamma) = \frac{\left\langle \phi_k^L(\gamma) \middle| \phi_k^R(\gamma) \right\rangle}{\left\langle \phi_k^R(\gamma) \middle| \phi_k^R(\gamma) \right\rangle} = \frac{1}{\left\langle \phi_k^R(\gamma) \middle| \phi_k^R(\gamma) \right\rangle}}$$

$\phi_k^R(\gamma)\ \phi_k^L(\gamma)$ normalized right (left) eigenvector

$$\boxed{a_{kl} = \left\langle \phi_l^L(0) \middle| \phi_k^R(\gamma) \right\rangle}$$

$\left\langle \tilde{\phi}_l^L(0) \right|$ the original state

$$\boxed{a'_{kl} = \left\langle \varphi_l \middle| \phi_k^R(\gamma) \right\rangle}$$

$\left\langle \varphi_l \right|$ the unit vector

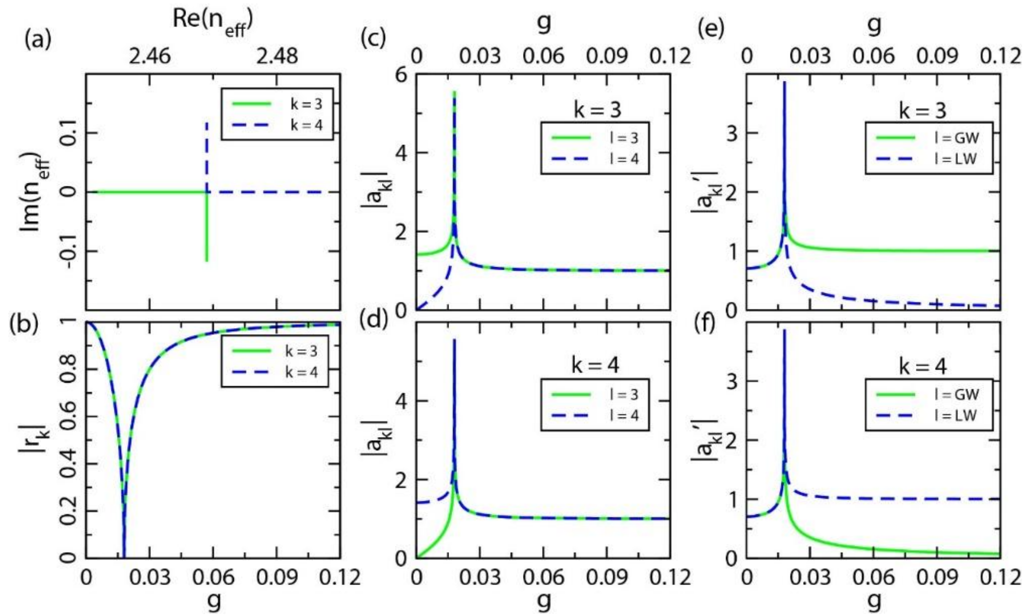

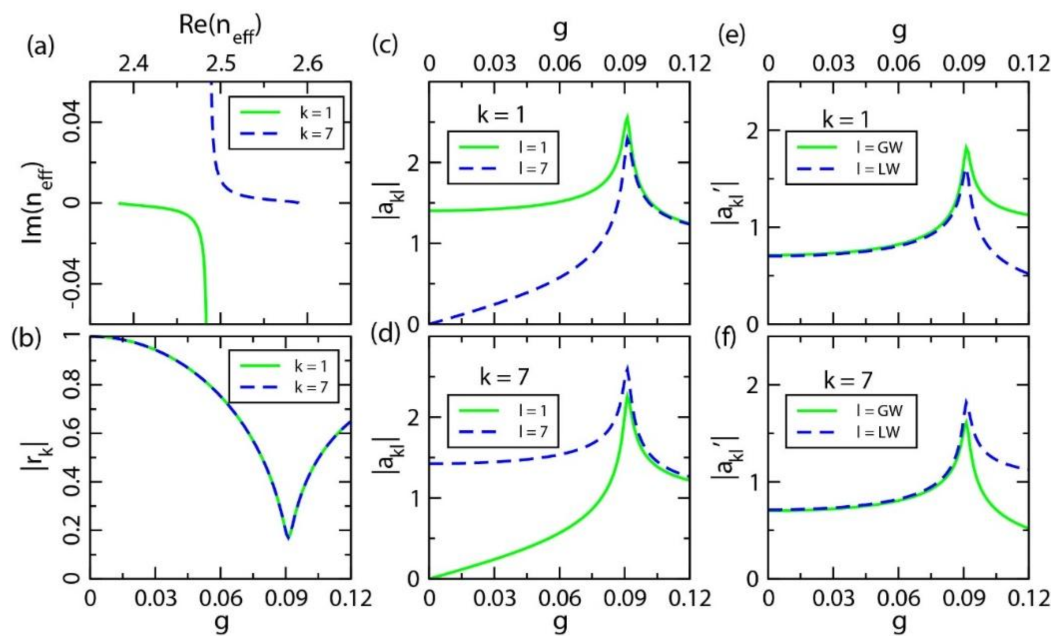

Our Interests

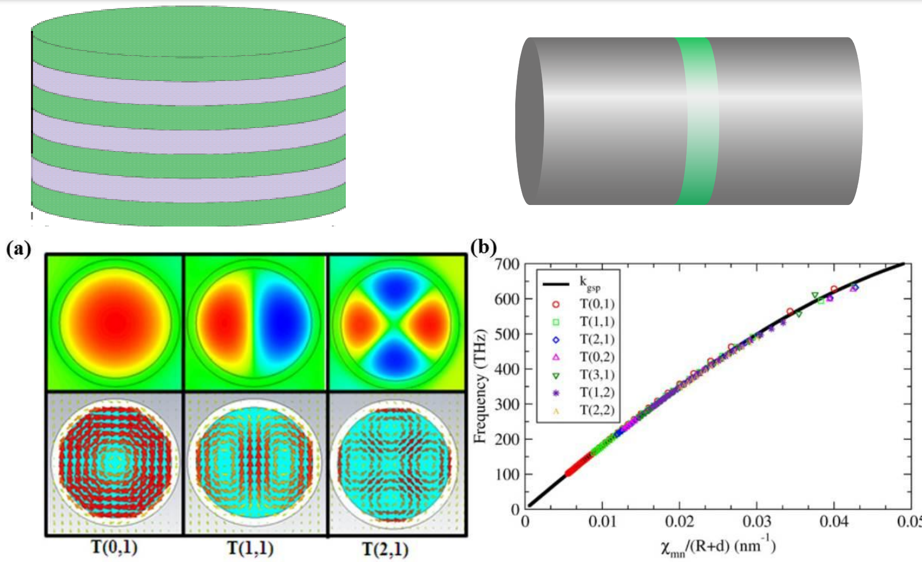

Photonic cavity and magnetic resonance modes

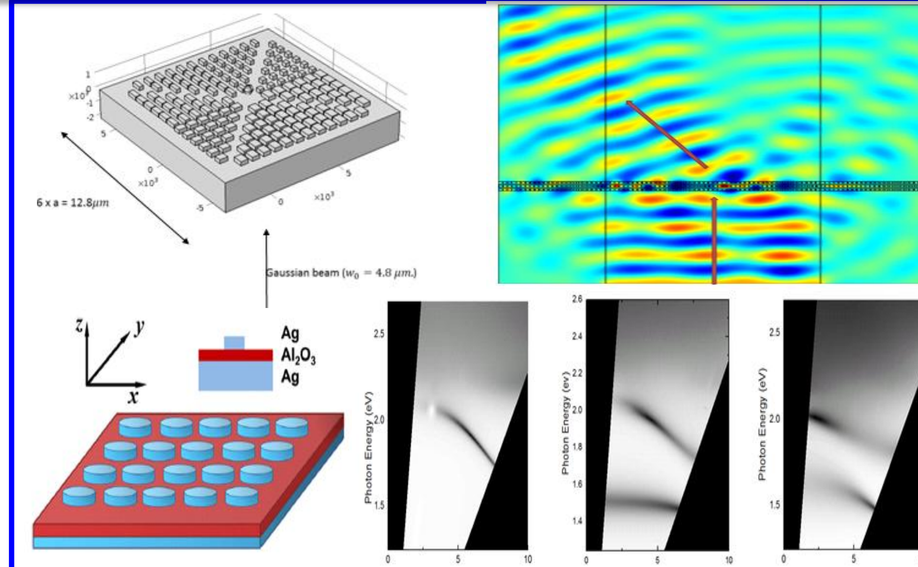

Metal-dielectric artificial metasurfaces

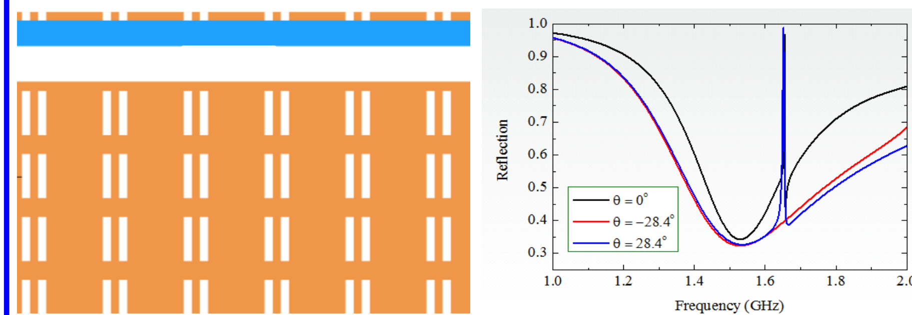

Magnetically controllable directional metasurface

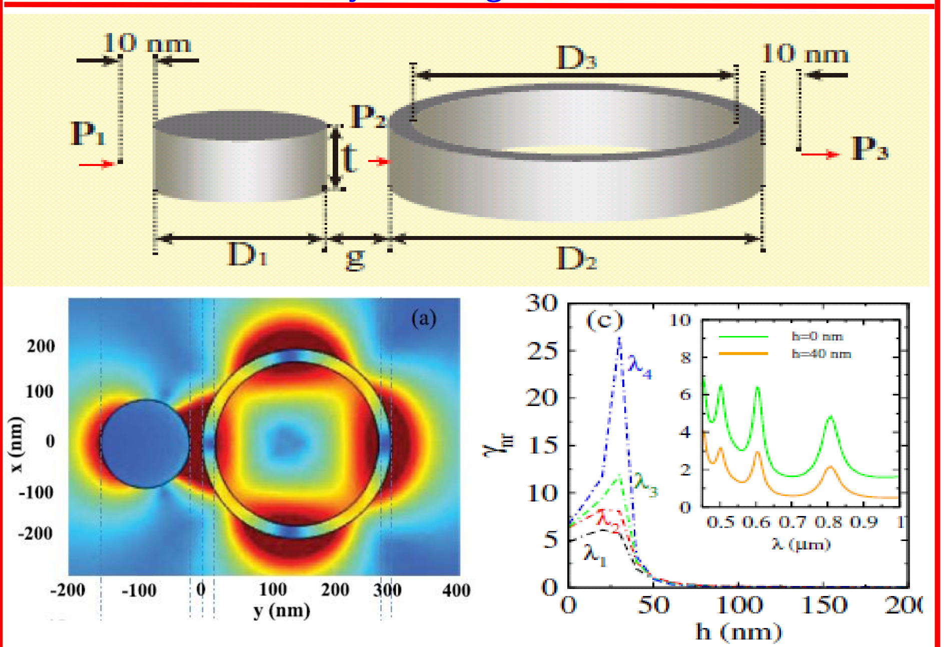

Nanoantenna and optical-matter interaction

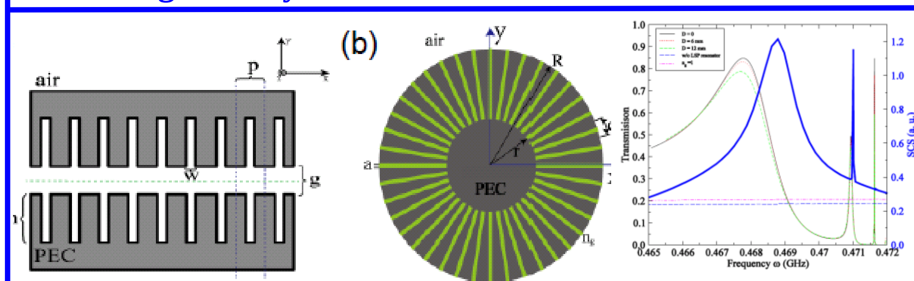

Spoof SPP resonator and waveguide

Acknowledgements

Financial Support

- NSFC(11004043, 11274083)
- 973 Program (2012CB921501)
- Guangdong Province NSF (2015A030313748)
- Shenzhen Municipal Science & Technology Plan (JCYJ20150513151706573, JSGG20150529153336124)
- Shenzhen Oversea Talent Plan (KQCX20120801093710373)

Group Member (Ph.D Candidates)


Q. Zhang


X. M. Zhang


Z. Z. Liu

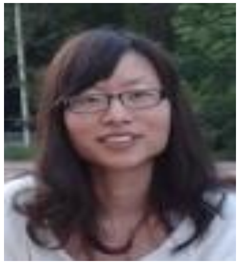
F. F. Qin

Collaborators

- Prof. K. W. Yu, Chinese University of Hong Kong
- Prof. D. Z. Han, Chongqing University
- Prof. L. Gao, Soochow University
- Prof. W. G. Liang, Fujian Inst. Res. Stuct. Matt.
- Prof. K. Y. Tao, Shenzhen University


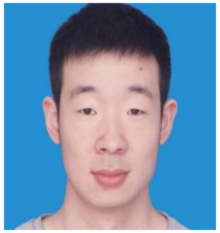




Master Students

5-year development plan of HIT@Shenzhen

Expanding…

哈尔滨工业大学（深圳） with PG & UG

师资队伍建设	教职员总体规模	1200 人
	专任教师数、生师比、职称结构比例、专任教师博士化率、有一年以上海外留学或工作经历的专任教师占教师总数比例	专任教师 600 人，生师比 12:1，博士化率 95%以上，有一年以上海外留学或工作经历的专任教师占教师总数 85%以上
	高端人才数（长江学者特聘教授、国家自然科学基金杰出青年基金获得者、千人计划、青年长江学者、青年千人计划、国家自然科学基金优秀青年基金获得者等）	100-120 人
	外籍教师数	100-120 人
	在站博士后数	150 人
	累计出站博士后数	350 人
	外籍博士后数	60 人

Thank you !